

# $A_4$ realization of left-right symmetric linear seesaw

Purushottam Sahu<sup>a1</sup>, Sudhanwa Patra<sup>a 2</sup>, Prativa Pritimita<sup>b3</sup>

<sup>a</sup>*Dept. of Physics, Indian Institute of Technology Bhilai, Raipur-492015, India,*

<sup>b</sup>*Dept. of Physics, Indian Institute of Technology Bombay, Powai, Mumbai-400076, India*

## Abstract

We explore an  $A_4$ -symmetric flavor based left-right symmetric model with linear seesaw mechanism and study the associated neutrino phenomenology. The framework offers the advantage of studying neutrino mass, non-unitarity effects in lepton sector, lepton flavour violation and CP violation. The fermion content of the model includes usual quarks, leptons along with additional sterile fermion per generation while the scalar content includes Higgs doublets and scalar bidoublet. We study analytically as well as numerically the correlation between different model parameters and their dependence on experimentally determined neutrino observables.

arXiv:2002.06846v1 [hep-ph] 17 Feb 2020

---

<sup>1</sup>purushottams@iitbhilai.ac.in

<sup>2</sup>sudhanwa@iitbhilai.ac.in

<sup>3</sup>prativa@iitb.ac.in

# 1 Introduction

The left-right symmetric model (LRSM) which was initially proposed as the most economical approach to restore parity came a long way in explaining neutrino mass, lepton number violation, dark matter, baryon asymmetry of the universe thereby gaining popularity [1–10]. All accolades to its gauge group, i.e.  $SU(3)_C \times SU(2)_L \times SU(2)_R \times U(1)_{B-L}$  which naturally gives room to a right handed neutrino and obeys a complete symmetry between left and right chirality until spontaneous symmetry breaking occurs. The model predicts  $W_R^\pm$  and  $Z'$  gauge bosons which couple to Standard Model fields and heavy Majorana neutrino  $N$  and these exotic states at low scale offer rich collider phenomenology. Neutrino mass can be explained within LRSM via various seesaw mechanisms like the canonical seesaw [11–18] and its lowscale variants like inverse seesaw [19], linear seesaw, extended seesaw etc [20]. The issue with canonical seesaw is that it links the smallness of neutrino mass to a very heavy right-handed scale which can't be verified by the current or planned experiments. Whereas in case of low scale seesaw heavy neutrino mass can lie in the TeV range which is experiment friendly and moreover it offers rich phenomenology like lepton flavor violation [21–25] and new physics contributions to lepton number violating decays like neutrinoless double beta decay [13, 26–50]. Inverse seesaw and linear seesaw can be realized with the introduction of extra singlet fermions per generation to the LRSM where the mass matrix in the basis  $(\nu_L, \nu_R^c, S_L)$  can be written as,

$$\mathbb{M} = \begin{pmatrix} 0 & m_D & m_{LS} \\ m_D^T & 0 & m_{RS} \\ m_{LS}^T & m_{RS}^T & \mu \end{pmatrix}. \quad (1.1)$$

Thus the light neutrino mass formula becomes,  $m_\nu^{\text{inv}} = \left(\frac{m_D}{m_{RS}}\right) \mu \left(\frac{m_D}{m_{RS}}\right)^T$  in the former case and  $m_\nu^{\text{lin}} = m_D m_{RS}^{-1} m_{LS}^T + \text{transpose}$  in the later case. It can be interpreted from the formula that it allows order one magnitude of Dirac Yukawa coupling, large light-heavy neutrino mixing and heavy neutrinos of mass few TeV. In [28], LRSM has been extended to study natural type-II seesaw dominance which allows large light-heavy neutrino mixing thus leading to many new physics contributions to neutrinoless double beta decay along with constraints on light neutrino mass. Another interesting variant is universal seesaw which allows all the quarks and leptons to get mass from a common seesaw due to the addition of vector-like fermions in LRSM [26].

However we aim to study here the  $A_4$  extension of LRSM which offers the advantage of studying neutrino mass, non-unitarity effect in linear seesaw, lepton flavour violation and CP violation within one framework.  $A_4$ , the discrete group of even permutations of four objects is the smallest non-Abelian group containing triplet irreducible representations. While it

was first proposed in [51] to study lepton masses and mixing, several other  $A_4$ -based flavour models have been suggested after that mostly to shed light on the flavour problem [52–55]. In one such recent work [56] the authors have elegantly explained the origin of non-zero  $\theta_{13}$  and leptogenesis via inverse seesaw with  $A_4$  extension of SM. However in the model the light-heavy neutrino mixing is proportional to identity and thus the branching ratios of LFV decays become vanishingly small. Similarly, another paper which considers realization of linear seesaw with  $A_4$  symmetry gives suppressed contributions to lepton flavour violating (LFV) decays due to the chosen model parameters [57]. This can be ameliorated by considering  $A_4$  realization of LRSM where large non-unitarity effect can be achieved and thus it can lead to dominant contributions to LFV decays, which is the primary motive of this work. The embedding of  $A_4$  group into left-right flavour symmetry has been attempted previously in order to explain charged fermion mass hierarchies and quark and lepton mixing angles [58, 59].

In this work, we have considered  $A_4$  realization of left-right symmetric linear seesaw mechanism. The fermion content of the model includes usual quarks, leptons along with additional sterile fermion per generation while the scalar content includes Higgs doublets with  $B - L = 1$  and scalar bidoublet with  $B - L = 0$ . Within this scenario all the fermion masses get simpler mass structure for neutrino phenomenology. While the right-handed Higgs doublet  $H_R$  plays the crucial role of left-right symmetry breaking, its left handed partner  $H_L$  has merely any role. Thus the non-zero VEV of  $H_L$  can be taken too small. As usual the scalar bidoublet  $\Phi$  plays the role of electroweak symmetry breaking. The introduction of  $A_4$  symmetry helps to avoid the  $\mu$  term and hence, inverse seesaw term for light neutrino masses is absent. The other good points of the model are large light-heavy neutrino mixing, prominent non-unitarity effects, dominant lepton flavour violating effects and CP-violating effects. The work also contains a number of plots showing correlation among model parameters and the experimentally observed parameters.

The paper is organised as follows. In Sec 2 we briefly note the features of manifest left-right symmetric model and then move to explain the realization of linear seesaw structure with  $A_4$  extension of the left-right model. In Sec 3 we discuss neutrino masses and mixing. We do so by setting up the flavour structure of neutrino mass matrices and establish analytically the correlation among model parameters. In Sec 4 we estimate numerically the correlation among model parameters by using the values of experimentally measured neutrino parameters. Sec 5 explains non-unitarity effects in linear seesaw and Sec 6 has a discussion on various low energy lepton flavour violating processes that the model facilitates. In Sec 7 we study leptonic CP violation for active neutrinos using Jarlskog invariants and in Sec 8 we summarize the work.

## 2 Left-right symmetric model with linear seesaw

The gauge group of left-right symmetric model (LRSM) is given by

$$SU(3)_C \times SU(2)_L \times SU(2)_R \times U(1)_{B-L} \quad (2.1)$$

where  $B - L$  stands for the difference between baryon number and lepton number. The standard lepton and quark content of the model is given by

$$\ell_L = \begin{pmatrix} \nu_L \\ e_L \end{pmatrix} \sim (1, 2, 1, -1), \quad \ell_R = \begin{pmatrix} \nu_R \\ e_R \end{pmatrix} \sim (1, 1, 2, -1) \quad (2.2)$$

$$q_L = \begin{pmatrix} u_L \\ d_L \end{pmatrix} \sim (3, 2, 1, \frac{1}{3}), \quad q_R = \begin{pmatrix} u_R \\ d_R \end{pmatrix} \sim (3, 1, 2, \frac{1}{3}). \quad (2.3)$$

The scalar sector of a general LRSM contains two Higgs doublets and a bidoublet

$$H_L = \begin{pmatrix} h_L^0 \\ h_L^- \end{pmatrix} \sim (1, 2, 1, -1), \quad H_R = \begin{pmatrix} h_R^0 \\ h_R^- \end{pmatrix} \sim (1, 1, 2, -1), \quad (2.4)$$

$$\Phi = \begin{pmatrix} \phi_1^0 & \phi_2^+ \\ \phi_1^- & \phi_2^0 \end{pmatrix} \sim (1, 2, 2, 0). \quad (2.5)$$

In order to generate neutrino mass through linear seesaw mechanism within LRSM, we will have to add one left-right gauge singlet neutral fermion  $S_L$  to the model. Now the complete Lagrangian for the leptonic sector becomes,

$$\begin{aligned} -\mathcal{L}_{\text{lepton}} &= \bar{\ell}_L (Y\Phi + \tilde{Y}\tilde{\Phi}) \ell_R \\ &\quad + Y_L \bar{\ell}_L H_L S_L + Y_R \bar{\ell}_R H_R S_L + h.c. \end{aligned} \quad (2.6)$$

Once the scalars  $H_L, H_R$  and  $\Phi$  obtain VEV as,

$$\langle H_L \rangle = \begin{pmatrix} 0 \\ v_L \end{pmatrix}, \quad \langle H_R \rangle = \begin{pmatrix} 0 \\ v_R \end{pmatrix}, \quad \langle \Phi \rangle = \begin{pmatrix} v_1 & 0 \\ 0 & v_2 \end{pmatrix}, \quad (2.7)$$

the above Lagrangian can be written as,

$$-\mathcal{L}_{\text{lepton}} = m_{LR} \bar{\nu}_L \nu_R + m_{RS} \bar{\nu}_R^c S_L + m_{LS} \bar{\nu}_L S_L + h.c. \quad (2.8)$$

Hence in the the basis  $(\nu_L, \nu_R^c, S_L)$ , the effective  $9 \times 9$  mass matrix can be written as

$$M_\nu = \begin{pmatrix} 0 & m_{LR} & m_{LS} \\ m_{LR}^T & 0 & m_{RS} \\ m_{LS}^T & m_{RS}^T & 0 \end{pmatrix}, \quad (2.9)$$

	Fields	$SU(3)_c$	$SU(2)_L$	$SU(2)_R$	$B - L$	$A_4$	$Z_4$	$Z_3$
	$\ell_{L1,2,3}$	<b>1</b>	<b>2</b>	<b>1</b>	-1	$1, 1'', 1'$	-1	1
	$\ell_R$	<b>1</b>	<b>1</b>	<b>2</b>	-1	3	$i$	1
	$S_L$	<b>1</b>	<b>1</b>	<b>1</b>	0	3	$i$	$\omega^2$
	$\Phi$	<b>1</b>	<b>2</b>	<b>2</b>	0	1	1	1
	$H_L$	<b>1</b>	<b>2</b>	<b>1</b>	-1	1	1	$\omega$
	$H_R$	<b>1</b>	<b>1</b>	<b>2</b>	-1	1	1	$\omega^2$
	$\phi_S$	<b>1</b>	<b>1</b>	<b>1</b>	0	3	-1	1
	$\phi_T$	<b>1</b>	<b>1</b>	<b>1</b>	0	3	$i$	1
	$\xi$	<b>1</b>	<b>1</b>	<b>1</b>	0	1	-1	1
	$\xi'$	<b>1</b>	<b>1</b>	<b>1</b>	0	$1'$	-1	1

Table 1: Particle content and transformation properties under  $A_4$  based flavour left-right symmetric model.

where  $m_{LR} = Y_1 v_1 + Y_2 v_2^*$  and  $m_{RS} = y_1 v_R$ . In the above matrix, one may wonder why the  $\mu$  term is absent, which will be clarified in the next section once we introduce  $A_4$  symmetry. Now, with  $m_{LS} \ll m_{LR} < m_{RS}$ , the light neutrino masses are obtained from the formula,

$$m_\nu = m_{LR} m_{RS}^{-1} m_{LS}^T + \text{transpose} \quad (2.10)$$

## 2.1 An $A_4$ realization of left-right symmetric linear seesaw mechanism

$A_4$  symmetry group has four irreducible representations; three singlets, namely  $1, 1', 1''$  and a triplet  $3$ . The multiplication rules for the irreducible representations can be written as;  $1 \otimes 1 = 1$ ,  $1' \otimes 1' = 1''$ ,  $1'' \otimes 1'' = 1'$ ,  $1' \otimes 1'' = 1$ . The product of two  $A_4$  triplets;  $(a_1, a_2, a_3)$  and  $(b_1, b_2, b_3)$  can be written as,

$$3 \times 3 = 1 + 1' + 1'' + 3_A + 3_S \quad (2.11)$$

$$\begin{aligned}
1 &\sim a_1 b_1 + a_2 b_3 + a_3 b_2 & (2.12) \\
1' &\sim a_3 b_3 + a_1 b_2 + a_2 b_2 \\
1'' &\sim a_2 b_2 + a_3 b_1 + a_1 b_3 \\
3_S &\sim \frac{1}{3} \begin{bmatrix} 2a_1 b_1 - a_2 b_3 - a_3 b_2 \\ 2a_3 b_3 - a_1 b_2 - a_2 b_1 \\ 2a_2 b_2 - a_1 b_3 - a_3 b_1 \end{bmatrix} \\
3_A &\sim \frac{1}{2} \begin{bmatrix} a_2 b_3 - a_3 b_2 \\ a_1 b_2 - a_2 b_1 \\ a_3 b_1 - a_1 b_3 \end{bmatrix}
\end{aligned}$$

With the particle content and symmetries mentioned in Table 1, the Lagrangian involved in generation of the mass matrices in a left-right  $A_4$  flavor symmetric framework can be written as,

$$-\mathcal{L}_{\text{lepton}} = \mathcal{L}_{\nu_L \nu_R} + \mathcal{L}_{\nu_R S_L} + \mathcal{L}_{\nu_L S_L}, \quad (2.13)$$

where

$$\begin{aligned}
\mathcal{L}_{\nu_L \nu_R} &= \frac{1}{\Lambda} (\overline{\ell_{L1}})_1 \left( Y \Phi + \tilde{Y} \tilde{\Phi} \right) (\ell_R \phi_T)_1 \\
&\quad + \frac{1}{\Lambda} (\overline{\ell_{L2}})_{1''} \left( Y \Phi + \tilde{Y} \tilde{\Phi} \right) (\ell_R \phi_T)_{1'} \\
&\quad + \frac{1}{\Lambda} (\overline{\ell_{L3}})_{1'} \left( Y \Phi + \tilde{Y} \tilde{\Phi} \right) (\ell_R \phi_T)_{1''}
\end{aligned} \quad (2.14)$$

With the vevs for the scalar and flavon fields as,  $\langle \phi_S \rangle = v_S(1, 1, 1)$ ,  $\langle \phi_T \rangle = v_T(1, 0, 0)$ ,  $\langle \xi \rangle = v_\xi$ ,  $\langle \xi' \rangle = v_{\xi'}$ , we obtain the flavor structures of the involved mass matrices.

$$M_\ell = \frac{v_T}{\Lambda} \begin{pmatrix} Y_{11} v_2 + \tilde{Y}_{11} v_1^* & 0 & 0 \\ 0 & Y_{22} v_2 + \tilde{Y}_{22} v_1^* & 0 \\ 0 & 0 & Y_{33} v_2 + \tilde{Y}_{33} v_1^* \end{pmatrix}. \quad (2.15)$$

In analogy to the charged lepton mass matrix, the Dirac mass for light neutrinos can be written as,

$$m_{LR} = \frac{v_T}{\Lambda} \begin{pmatrix} Y_{11} v_1 + \tilde{Y}_{11} v_2^* & 0 & 0 \\ 0 & Y_{22} v_1 + \tilde{Y}_{22} v_2^* & 0 \\ 0 & 0 & Y_{33} v_1 + \tilde{Y}_{33} v_2^* \end{pmatrix} \quad (2.16)$$

$$= \frac{v_T}{\Lambda} Y_D v \begin{pmatrix} 1 & 0 & 0 \\ 0 & 1 & 0 \\ 0 & 0 & 1 \end{pmatrix}, \quad (2.17)$$

where we have considered,  $Y_D v \equiv Y v_1 + \tilde{Y} v_2^* = Y_{11,22,33} v_1 + \tilde{Y}_{11,22,33} v_2^*$ .

It is seen from Table-1 that under  $A_4$ ,  $\ell_L$  transforms as 1, 1', 1'' for 1st, 2nd and 3rd generation of left-handed doublet respectively,  $S_L$  transforms as triplet and  $H_L, H_R$  as singlets. Thus the  $\nu_L - S_L$  mixing term;  $\bar{\ell}_L^c H_L S_L$  and the  $\nu_R - S_L$  mixing term  $\bar{\ell}_R H_R S_L$  are not allowed at tree level and are generated at dimension five level as follows,

$$\begin{aligned} \mathcal{L}_{\nu_L S_L} &= \frac{Y_L^{11}}{\Lambda} (\bar{\ell}_{L1})_1 H_L (S_L \phi_T)_1 \\ &+ \frac{Y_L^{22}}{\Lambda} (\bar{\ell}_{L2})_{1''} H_L (S_L \phi_T)_{1'} \\ &+ \frac{Y_L^{33}}{\Lambda} (\bar{\ell}_{L3})_{1'} H_L (S_L \phi_T)_{1''} \end{aligned} \quad (2.18)$$

Once  $\langle H_L \rangle$  and  $\langle \phi_T \rangle$  get vev, the  $\nu_L - S_L$  mixing matrix becomes,

$$m_{LS} = \frac{v_T}{\Lambda} \begin{pmatrix} Y_L^{11} v_L & 0 & 0 \\ 0 & Y_L^{22} v_L & 0 \\ 0 & 0 & Y_L^{33} v_L \end{pmatrix} \quad (2.19)$$

$$= \frac{v_T}{\Lambda} Y_L v_L \begin{pmatrix} 1 & 0 & 0 \\ 0 & 1 & 0 \\ 0 & 0 & 1 \end{pmatrix}, \quad (2.20)$$

where we have considered,  $Y_L v_L = Y_L^{11,22,33} v_L$ . As we have mentioned earlier, the scalar  $H_R$  plays the crucial role of left-right symmetry breaking, and  $H_L$  is required only for left-right invariance. Thus  $H_L$  gets a small induced vev which is much smaller than  $H_R$ . This clarifies why  $m_{LS}$  term is much smaller than the  $m_{RS}$  term.

Similarly, the  $\nu_R - S_L$  mixing term is generated at dimension five level as follows

$$\mathcal{L}_{\nu_R S_L} = \frac{1}{\lambda} \left( \lambda^{\phi_s} \phi_s + \lambda^\xi \xi + \lambda^{\xi'} \xi' \right) \bar{\ell}_R H_R S_L. \quad (2.21)$$

The advantage of forbidding  $\bar{\nu}_L - S_L$  and  $\bar{\nu}_R - S_L$  terms at tree level and generating them by dimension five operator is that it helps in achieving large light-heavy neutrino mixing which gives large non-unitarity effects and lepton flavour violation. It should be noted that the terms  $\mathcal{L}_{\nu_L \nu_R}$ ,  $\mathcal{L}_{\nu_L S_L}$  and  $\mathcal{L}_{\nu_R S_L}$  represent the contributions for Dirac neutrino mass connecting  $\nu_L - \nu_R$ ,  $\nu_L - S_L$ ,  $\nu_R - S_L$  mixing, respectively. If one looks at the mass formula for light neutrinos governed by linear seesaw mechanism given in Eq.2.10, one can use the mass hierarchy  $m_{RS} \gg m_{LR}, m_{LS}$ .

Using the following vevs for the scalar and flavon fields

$$\langle \phi_S \rangle = v_S (1, 1, 1), \langle \phi_T \rangle = v_T (1, 0, 0), \langle \xi \rangle = v_\xi, \langle \xi' \rangle = v_{\xi'}, \quad (2.22)$$

the various mass matrices are found to be,

$$m_{LR} = \frac{Y_D v v_T}{\Lambda} \begin{pmatrix} 1 & 0 & 0 \\ 0 & 1 & 0 \\ 0 & 0 & 1 \end{pmatrix}, \quad m_{LS} = \frac{Y_L v_L v_T}{\Lambda} \begin{pmatrix} 1 & 0 & 0 \\ 0 & 1 & 0 \\ 0 & 0 & 1 \end{pmatrix}, \quad (2.23)$$

$$m_{RS} = \frac{a}{3} \begin{pmatrix} 2 & -1 & -1 \\ -1 & 2 & -1 \\ -1 & -1 & 2 \end{pmatrix} + b \begin{pmatrix} 1 & 0 & 0 \\ 0 & 0 & 1 \\ 0 & 1 & 0 \end{pmatrix} + d \begin{pmatrix} 0 & 0 & 1 \\ 0 & 1 & 0 \\ 1 & 0 & 0 \end{pmatrix}, \quad (2.24)$$

where  $a = \lambda^\phi v_S v_R / \Lambda$ ,  $b = \lambda^\xi v_\xi v_R / \Lambda$  and  $d = \lambda^{\xi'} v_{\xi'} v_R / \Lambda$ .

### 3 Neutrino Masses and Mixing

In this section we focus on studying the correlation between different model parameters and their dependence on experimentally determined neutrino parameters. We start by rewriting the mass matrix  $m_{RS}$  (2.24) for calculational convenience as,

$$m_{RS} = \begin{pmatrix} 2a/3 + b & -a/3 & -a/3 \\ -a/3 & 2a/3 & -a/3 + b \\ -a/3 & -a/3 + b & 2a/3 \end{pmatrix} + \begin{pmatrix} 0 & 0 & d \\ 0 & d & 0 \\ d & 0 & 0 \end{pmatrix}. \quad (3.1)$$

The importance of this matrix is that it dictates the flavour structure of the light neutrino mass matrix  $m_\nu$  in the linear seesaw scenario. Moreover, the structure of this matrix is such that, it leads to lepton mixing consistent with neutrino oscillation data [60,61].

Using Eqns.(2.22),(2.23) and (2.24), one can write the light neutrino mass matrix as,

$$\begin{aligned} m_\nu &= m_{LR} m_{RS}^{-1} m_{LS}^T + \text{transpose} \\ &= k_1 k_2 \begin{pmatrix} 1 & 0 & 0 \\ 0 & 1 & 0 \\ 0 & 0 & 1 \end{pmatrix} m_{RS}^{-1} \begin{pmatrix} 1 & 0 & 0 \\ 0 & 1 & 0 \\ 0 & 0 & 1 \end{pmatrix}, \end{aligned} \quad (3.2)$$

where the parameters  $k_1$  and  $k_2$  are related to the vevs through

$$k_1 = \sqrt{2} Y_D v \frac{v_T}{\Lambda}, \quad k_2 = \sqrt{2} Y_L v_L \frac{v_T}{\Lambda}.$$

The inverse of light neutrino mass matrix becomes,

$$m_\nu^{-1} = \frac{1}{k_1 k_2} \begin{pmatrix} 2a/3 + b & -a/3 & -a/3 \\ -a/3 & 2a/3 & -a/3 + b \\ -a/3 & -a/3 + b & 2a/3 \end{pmatrix} + \frac{1}{k_1 k_2} \begin{pmatrix} 0 & d & 0 \\ d & 0 & 0 \\ 0 & 0 & d \end{pmatrix}, \quad (3.3)$$



which in TBM [62–64] basis will have the form, i.e.,  $m_\nu^{-1'} = U_{\text{TBM}}^T m_\nu^{-1} U_{\text{TBM}}$ ,

$$m_\nu^{-1'} = \begin{pmatrix} a + b - d/2 & 0 & -\frac{\sqrt{3}}{2}d \\ 0 & b + d & 0 \\ -\frac{\sqrt{3}}{2}d & 0 & a - b + d/2 \end{pmatrix}. \quad (3.4)$$

The above matrix  $m_\nu^{-1'}$  can be diagonalized by  $U_{13}^*$ . Which means  $m_\nu^{-1}$  can be diagonalized by  $U_{\text{TBM}} \cdot U_{13}^*$  and  $m_\nu$  by  $U_{\text{TBM}} \cdot U_{13}$ , while  $m_{RS}$  by  $U_{\text{TBM}} \cdot U_{13}^T$ . The matrix  $U_{13}$  and  $U_{\text{TBM}}$  are of the form

$$U_{\text{TBM}} = \begin{pmatrix} \sqrt{\frac{2}{3}} & \sqrt{\frac{1}{3}} & 0 \\ -\sqrt{\frac{1}{6}} & \sqrt{\frac{1}{3}} & \sqrt{\frac{1}{2}} \\ -\sqrt{\frac{1}{6}} & \sqrt{\frac{1}{3}} & -\sqrt{\frac{1}{2}} \end{pmatrix}, \quad (3.5)$$

$$U_{13} = \begin{pmatrix} \cos \theta & 0 & \sin \theta e^{-i\delta} \\ 0 & 1 & 0 \\ -\sin \theta e^{i\delta} & 0 & \cos \theta \end{pmatrix}, \quad (3.6)$$

where internal mixing angle  $\theta$  and phase  $\delta$  are expressed in terms of the mass matrix parameters  $d/b = \lambda_1 e^{\phi_{ab}}$ ,  $a/b = \lambda_2 e^{\phi_{ab}}$  as

$$\tan 2\theta = -\frac{\sqrt{3}\lambda_1 \cos \phi_{db}}{(\lambda_1 \cos \phi_{db} - 2) \cos \delta + (2\lambda_2 \sin \phi_{ab}) \sin \delta}, \quad (3.7)$$

and

$$\tan \delta = \frac{\sin \phi_{db}}{\lambda_2 \cos(\phi_{ab} - \phi_{db})}. \quad (3.8)$$

The purpose of rotating the  $m_\nu$  matrix by  $U_{\text{TBM}}$  followed by  $U_{13}$  is to achieve non-zero reactor mixing angle  $\theta_{13}$  and see the possible correlations between various parameters.

Again, from Eq.3.1 and 3.2 it is found that eigenvalues of  $m_\nu$  and  $m_{RS}$  are related to each other as

$$m_i = \frac{k_1 k_2}{M_i}. \quad (3.9)$$

where  $m_i$  and  $M_i$  are  $i^{\text{th}}$  eigenvalues of  $m_\nu$  and  $m_{RS}$  respectively. The eigenvalues of  $m_{RS}$  can be expressed using defined parameters in terms of  $\lambda_1$  and  $\lambda_2$  as,

$$\begin{aligned} M_1 &= b \left[ \lambda_2 e^{i\phi_{ab}} - \sqrt{1 + \lambda_1^2 e^{2i\phi_{db}} - \lambda_1 e^{i\phi_{db}}} \right], \\ M_2 &= b \left[ 1 + \lambda_1 e^{i\phi_{db}} \right], \\ M_3 &= b \left[ \lambda_2 e^{i\phi_{ab}} + \sqrt{1 + \lambda_1^2 e^{2i\phi_{db}} - \lambda_1 e^{i\phi_{db}}} \right], \end{aligned} \quad (3.10)$$

After some simple calculations, one can write the heavy neutrino masses as

$$\begin{aligned}
M_1 &= |b| [(\lambda_2 \cos \phi_{ab} - C)^2 + (\lambda_2 \sin \phi_{ab} - D)^2]^{1/2}, \\
M_2 &= |b| [1 + \lambda_1^2 + 2\lambda_1 \cos \phi_{db}]^{1/2}, \\
M_3 &= |b| [(\lambda_2 \cos \phi_{ab} + C)^2 + (\lambda_2 \sin \phi_{ab} + D)^2]^{1/2},
\end{aligned} \tag{3.11}$$

where

$$\begin{aligned}
C &= \left[ \frac{A + \sqrt{A^2 + B^2}}{2} \right]^{1/2}, & D &= \left[ \frac{-A + \sqrt{A^2 + B^2}}{2} \right]^{1/2}, \\
A &= 1 + \lambda_1^2 \cos 2\phi_{db} - \lambda_1 \cos \phi_{db}, & B &= \lambda_1^2 \sin 2\phi_{db} - \lambda_1 \sin \phi_{db}.
\end{aligned} \tag{3.12}$$

and the phases ( $\phi_i$ 's) of  $M_i$ , i.e.,  $M_i = |M_i|e^{i\phi_i}$  as

$$\begin{aligned}
\phi_1 &= \tan^{-1} \left[ \frac{\lambda_2 \sin \phi_{ab} - D}{\lambda_2 \cos \phi_{ab} - C} \right], \\
\phi_2 &= \tan^{-1} \left[ \frac{\lambda_1 \sin \phi_{db}}{1 + \lambda_1 \cos \phi_{db}} \right], \\
\phi_3 &= \tan^{-1} \left[ \frac{\lambda_2 \sin \phi_{ab} + D}{\lambda_2 \cos \phi_{ab} + C} \right].
\end{aligned} \tag{3.13}$$

The matrix which diagonalizes active neutrino mass matrix,  $U_\nu$  is given by

$$U_\nu = U_{TBM} \cdot U_{13} \cdot P, \tag{3.14}$$

with  $P = \text{diag}(e^{-i\phi_1/2}, e^{-i\phi_2/2}, e^{-i\phi_3/2})$ .

and the lepton mixing matrix, known as PMNS matrix is given by [65,66]

$$U_{\text{PMNS}} = U_\ell^\dagger \cdot U_\nu, \tag{3.15}$$

Here  $U_\ell = \mathbb{I}$ , which implies,

$$U_{\text{PMNS}} = U_{TBM} \cdot U_{13} \cdot P, \tag{3.16}$$

and this looks to be in good agreement with the experimental observations [67,68]. The PMNS matrix can be parametrized in terms of three mixing angles ( $\theta_{13}$ ,  $\theta_{23}$  and  $\theta_{12}$ ) and three phases (one Dirac phase  $\delta_{CP}$ , and two Majorana phases  $\rho$  and  $\sigma$ ) as

$$U_{\text{PMNS}} = \begin{pmatrix} c_{12}c_{13} & s_{12}c_{13} & s_{13}e^{-i\delta_{CP}} \\ -s_{12}c_{23} - c_{12}s_{13}s_{23}e^{i\delta_{CP}} & c_{12}c_{23} - s_{12}s_{13}s_{23}e^{i\delta_{CP}} & c_{13}s_{23} \\ s_{12}s_{23} - c_{12}s_{13}c_{23}e^{i\delta_{CP}} & -c_{12}s_{23} - s_{12}s_{13}c_{23}e^{i\delta_{CP}} & c_{13}c_{23} \end{pmatrix} P_\nu, \tag{3.17}$$

where  $c_{ij} = \cos \theta_{ij}$  and  $s_{ij} = \sin \theta_{ij}$  and  $P_\nu = \text{diag}(1, e^{i\rho/2}, e^{i\sigma/2})$ . From Eqns. (3.16) and (3.17), one can find

$$\begin{aligned} \sin \theta &= \sqrt{\frac{3}{2}} \sin \theta_{13} , \\ \sin \delta_{\text{CP}} &= -\frac{\sin \delta}{\sqrt{1 - \frac{3(2 - 3 \sin^2 \theta_{13})}{(1 - \sin^2 \theta_{13})^2} \sin^2 \theta_{13} \cos^2 \delta}} \approx -\sin \delta . \end{aligned} \quad (3.18)$$

The advantage of expressing  $\theta$  and  $\delta$  in this manner is that they become related to the mixing observables  $\sin^2 \theta_{13}$  and  $\delta_{\text{CP}}$  respectively.  $\sin^2 \theta_{13}$  is known more precisely than  $\delta_{\text{CP}}$ , and thus in our calculation we fix  $\theta$  by taking the best fit value of  $\sin^2 \theta_{13}$  and consider all possible values of  $\delta$  for which  $\delta_{\text{CP}}$  falls within its  $3\sigma$  experimental range. Even though the solar mixing angle lies slightly on the higher side of the observed central value in this case, i.e.,  $\sin^2 \theta_{12} = 1/(3 - 2 \sin^2 \theta)$ , it is still within the  $3\sigma$  range of the observed data.

## 4 Numerical results

In the previous section we set up the flavour structure of neutrino mass matrices and analytically established correlation among model parameters by fixing  $\delta$ ,  $\theta$  and other parameters like  $\phi_{ab}$ ,  $\phi_{db}$ . In this section, we intend to estimate numerically the inter-relation among the model parameters by using the measured values of the ratio of two mass squared differences,  $r$  and the different mixing angles,  $\theta_{12}$ ,  $\theta_{13}$ ,  $\theta_{23}$ . From Eqns. (3.9) the light neutrino masses are found to be

$$m_i = \frac{|k_1 k_2|}{M_i} . \quad (4.1)$$

Since the solar mass squared difference,  $\Delta m_{21}^2$  and atmospheric mass squared difference,  $|\Delta m_{32}^2|$  are measured in neutrino oscillation experiments, we calculate the mass squared differences from Eqn. (4.1) as,

$$\begin{aligned} \Delta m_{21}^2 &= \left| \frac{k_1 k_2}{b} \right|^2 \left( \frac{1}{M_2^2} - \frac{1}{M_1^2} \right) , \\ |\Delta m_{31}^2| &= \left| \frac{k_1 k_2}{b} \right|^2 \left| \left( \frac{1}{M_3^2} - \frac{1}{M_1^2} \right) \right| . \end{aligned} \quad (4.2)$$

In order to find the ratio of the two mass squared differences, ( $r$ ), one may substituting the set of Eqns. (3.11) in the above equations, so that

$$\begin{aligned} r &= \frac{\Delta m_{21}^2}{|\Delta m_{31}^2|} = \left[ \frac{(\lambda_2 \cos \phi_{ab} + C)^2 + (\lambda_2 \sin \phi_{ab} + D)^2}{1 + \lambda_1^2 + 2\lambda_1 \cos \phi_{db}} \right] \\ &\times \left[ \frac{(\lambda_2 \cos \phi_{ab} - C)^2 + (\lambda_2 \sin \phi_{ab} - D)^2 - (1 + \lambda_1^2 + 2\lambda_1 \cos \phi_{db})}{4\lambda_2 |C \cos \phi_{ab} + D \sin \phi_{ab}|} \right] . \end{aligned} \quad (4.3)$$

Now using Eqs. (3.7), (3.8), (3.11), (3.12) and (4.3), and by fixing the parameters  $\phi_{db}$ ,  $\delta$  and  $\theta$ , one can find numerical values of  $M_i$ . Once  $M_i$  are known  $\left| \frac{k_1 k_2}{b} \right|$  can be calculated from (4.2) as

$$\left| \frac{k_1 k_2}{b} \right| = \sqrt{\frac{\Delta m_{21}^2}{\left(\frac{1}{M_2^2} - \frac{1}{M_1^2}\right)}} = \sqrt{\left| \frac{\Delta m_{31}^2}{\left(\frac{1}{M_3^2} - \frac{1}{M_1^2}\right)} \right|}, \quad (4.4)$$

which will also give the absolute value of light neutrino masses as all the quantities on the right hand side of (4.1) are now known.

We now rewrite the expression  $\tan \delta$  Eq(3.8) in terms of  $\phi_{db}$  as

$$\phi_{db} = 0, \pi, \quad \text{for } \tan \delta = 0, \quad (4.5)$$

and

$$\phi_{ab} = \phi_{db} + \cos^{-1} \left( \frac{\sin \phi_{db}}{\lambda_2 \tan \delta} \right), \quad \text{for } \tan \delta \neq 0, \quad (4.6)$$

and consider the following cases to see the implications.

#### 4.1 Correlation between model parameters with $\tan \delta = 0$

The input model parameters for neutrino mass analysis are,

$$\lambda_1, \lambda_2, \phi_{db}, \phi_{ab}, \delta$$

For simplification, we chose  $\tan \delta = 0$  and  $\phi_{db}$  will be taken either 0 or  $\pi$ .

Case-I-  $\tan \delta = 0, \phi_{db} = 0$ ;

From eq. (3.7), the expressions that relates  $\lambda_1$  with internal mixing angle  $\theta$  is,

$$\lambda_1 = \frac{2 \tan 2\theta}{\sqrt{3} + \tan 2\theta}, \quad (4.7)$$

The ratio of the mass square differences  $r$  (4.3), satisfies the relation

$$r = \left[ \frac{\lambda_2^2 + 2\lambda_2 C \cos \phi_{ab} + C^2}{(1 + \lambda_1)^2} \right] \left[ \frac{\lambda_2^2 - 2\lambda_2 C \cos \phi_{ab} + C^2 - (1 + \lambda_1)^2}{4\lambda_2 |C \cos \phi_{ab}|} \right],$$

where,  $C = \sqrt{\frac{1 - \lambda_1 + \lambda_1^2}{2}}$ . (4.8)

The physical mass eigenvalues of  $m_{RS}$  in this case become

$$\begin{aligned} M_1 &= |b| \sqrt{\lambda_2^2 - 2\lambda_2 C \cos \phi_{ab} + C^2}, \\ M_2 &= |b|(1 + \lambda_1), \\ M_3 &= |b| \sqrt{\lambda_2^2 + 2\lambda_2 C \cos \phi_{ab} + C^2}. \end{aligned} \quad (4.9)$$

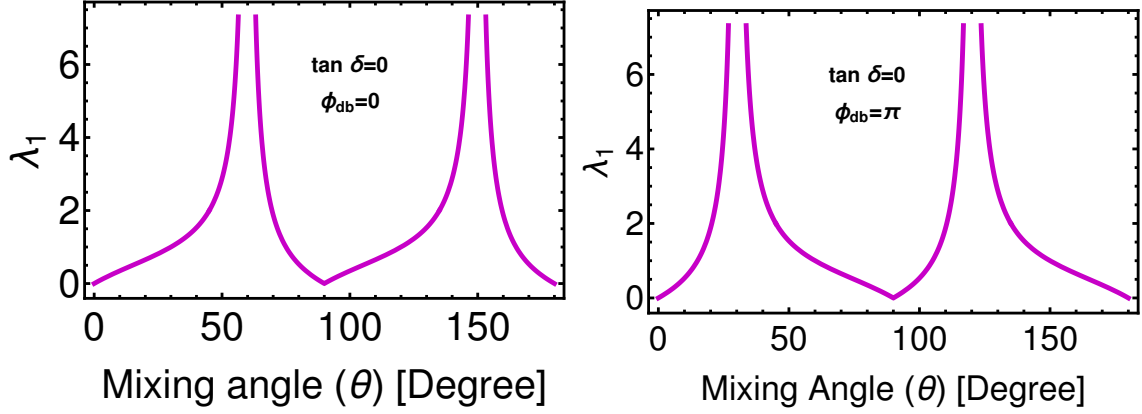


Figure 1: Plots for variation of  $\lambda_1$  and internal mixing angle  $\theta$  with  $\tan \delta = 0$  and  $\phi_{db} = 0$  (left panel),  $\phi_{db} = \pi$  (right panel).

Fig.1 displays variation of input model parameter  $\lambda_1$  with change in internal mixing angle  $\theta$  in the range 0 to 180 degree. It is seen from the figures that those values of  $\theta$  which are multiples of  $\frac{\pi}{4}$  are divergent or not allowed. The figures are plotted using equations (4.7) and (4.10) and it comes out that the figures are mirror images of each other due to the ‘+ve’ and ‘-ve’ signs of  $\tan 2\theta$  in the denominators of the respective equations. In Fig.2 using eq.(4.8) it is shown that input model parameters with  $\phi_{db} = 0$ ,  $\tan \delta = 0$  and variation of phase angle  $\phi_{ab}$  from  $0 - 2\pi$  are consistent with experiment measured value of  $r = 0.03$  [60]. In right-panel of Fig.2, it is shown that the ratio is divergent for  $\phi_{ab}$  around 90 degree, which means  $\phi_{ab}$  around 90 degree is not allowed. If we examine  $\phi_{ab}$  from two different ranges,  $0 - \pi$  to  $0 - 2\pi$  it is observed that for both case I and II the values of  $\phi_{ab}$  around  $(2n + 1)\frac{\pi}{2}$ ,  $n = 1, 2, 3, \dots$  are not allowed since at these values  $r$  diverges. So the constraints obtained on  $\phi_{ab}$  is that  $\phi_{ab} \neq (2n + 1)\frac{\pi}{2}$ .

**Case-II-** $\tan \delta = 0$ ,  $\phi_{db} = \pi$

For this case the relation between  $\lambda_1$  and  $\theta$  becomes,

$$\lambda_1 = \frac{2 \tan 2\theta}{\sqrt{3} - \tan 2\theta}, \quad (4.10)$$

and  $r$  obeys the relation

$$r = \left[ \frac{\lambda_2^2 + 2\lambda_2 C \cos \phi_{ab} + C^2}{(1 - \lambda_1)^2} \right] \times \left[ \frac{\lambda_2^2 - 2\lambda_2 C \cos \phi_{ab} + C^2 - (1 - \lambda_1)^2}{4\lambda_2 |C \cos \phi_{ab}|} \right], \quad (4.11)$$

with  $C = \sqrt{\frac{1 + \lambda_1 + \lambda_1^2}{2}}$ .

The eigenvalues of  $m_{RS}$  can be written as

$$\begin{aligned} M_1 &= |b| \sqrt{\lambda_2^2 - 2\lambda_2 C \cos \phi_{ab} + C^2}, \\ M_2 &= |b|(1 - \lambda_1), \\ M_3 &= |b| \sqrt{\lambda_2^2 + 2\lambda_2 C \cos \phi_{ab} + C^2}. \end{aligned} \quad (4.12)$$

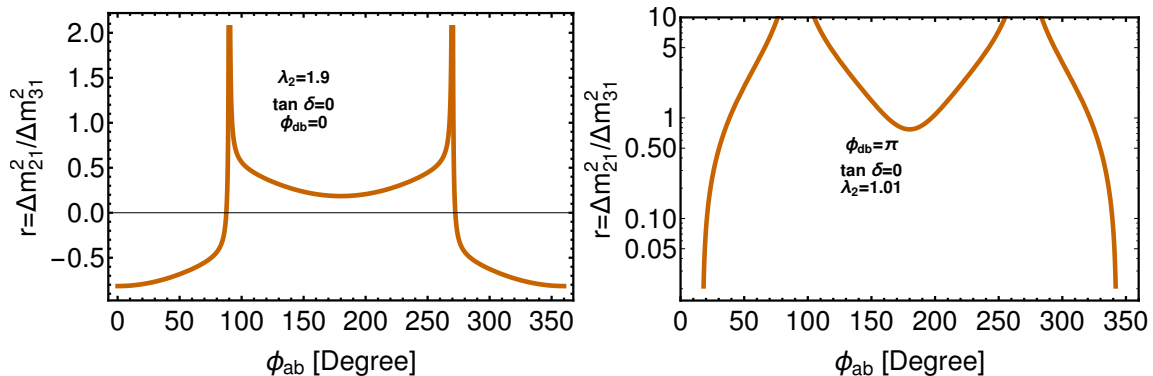


Figure 2: Contour plots for ratio of mass squared difference,  $r$  and  $\phi_{ab}$  from 0 to  $\pi$  with  $\phi_{db} = 0$  (left panel) and  $\phi_{db} = \pi$  (right panel) In these plots  $\phi_{ab}$  is taken from 0 to  $2\pi$

For the above two cases we have shown the correlation plots in Fig.1. It should be noted from (4.8) that  $r$  will be divergent near  $\phi_{ab} = \pi/2$  and thus, the values of  $\phi_{ab}$  around  $\pi/2$  are not allowed.

Similarly we can find Correlation between model parameters with  $\tan \delta \neq 0$ . In this case The analytic expression for  $\lambda_1$  is given by

$$\lambda_1 = \frac{2\lambda_2 \tan 2\theta \cos \phi_{ab} \sin \phi}{\sin \phi_{ab} [\sqrt{3} + \tan 2\theta \cos \phi]} . \quad (4.13)$$

## 4.2 Analysis on Neutrino mixing angles

In the present left-right symmetric model with linear seesaw mechanism, the light neutrino masses are diagonalized by  $\mathbb{U}_{\text{TBM}}$ ,  $\mathbb{U}_{13}$  containing the mixing angle  $\theta$  and phases. The form of the mixing matrix is expressed in terms of  $\theta$ ,  $\delta$  and other phases in the following way [56, 57, 69, 70],

$$\mathbb{U} = \begin{pmatrix} \frac{2}{\sqrt{6}} \cos \theta & \frac{1}{\sqrt{3}} & \frac{2}{\sqrt{6}} \sin \theta e^{-i\delta} \\ -\frac{1}{\sqrt{6}} \cos \theta + \frac{1}{\sqrt{2}} \sin \theta e^{i\delta} & \frac{1}{\sqrt{3}} & -\frac{1}{\sqrt{6}} \sin \theta e^{-i\delta} - \frac{1}{\sqrt{2}} \cos \theta \\ -\frac{1}{\sqrt{6}} \cos \theta - \frac{1}{\sqrt{2}} \sin \theta e^{i\delta} & \frac{1}{\sqrt{3}} & -\frac{1}{\sqrt{6}} \sin \theta e^{-i\delta} + \frac{1}{\sqrt{2}} \cos \theta \end{pmatrix} \cdot \begin{pmatrix} 1 & 0 & 0 \\ 0 & e^{i\frac{\alpha}{2}} & 0 \\ 0 & 0 & e^{i\frac{\beta}{2}} \end{pmatrix} .$$

where  $\alpha$  and  $\beta$  are the two Majorana phases.

The neutrino mixing angles like solar mixing angle  $\theta_{12}$ , atmospheric mixing angle  $\theta_{23}$ , reactor mixing angle  $\theta_{13}$  and Dirac CP-phase are related to the elements of the  $U_{\text{PMNS}}$  through the following set of equations  $\sin^2 \theta_{13} = |\mathbb{U}_{e3}|^2$ ,  $\sin^2 \theta_{12} = \frac{|\mathbb{U}_{e2}|^2}{1 - |\mathbb{U}_{e3}|^2}$ ,  $\tan^2 \theta_{23} = \frac{|\mathbb{U}_{\mu 3}|^2}{1 - |\mathbb{U}_{e3}|^2}$ . The final expressions for these mixing angles can also be expressed in terms of the model parameters like internal mixing angle  $\theta$  and phase  $\delta$  as,

$$\sin^2 \theta_{13} = \frac{2}{3} \sin^2 \theta, \sin^2 \theta_{12} = \frac{1}{2 + \cos 2\theta}, \sin^2 \theta_{23} = \frac{1}{2} \left( 1 + \frac{\sqrt{3} \sin 2\theta \cos \delta}{2 + \cos 2\theta} \right).$$

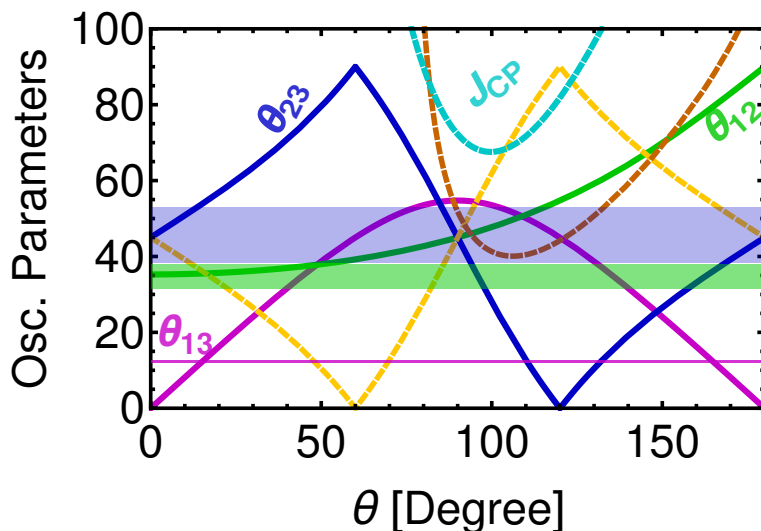


Figure 3: Variation of measured neutrino oscillation parameters like solar mixing angle ( $\theta_{12}$ ), reactor mixing angle ( $\theta_{13}$ ), and atmospheric mixing angle ( $\theta_{23}$ ) with the change of internal mixing angle  $\theta$  by fixing phase  $\delta$ .

The other known quantity in neutrino sector is Jarlskog rephrasing invariant [71] which can be expressed in terms  $\theta$  and  $\delta$  as,

$$J_{\text{CP}} = \text{Im} \left[ U_{e1} U_{\mu 2} U_{e2}^* U_{\mu 1}^* \right] = \frac{\sin \theta_{13}}{3\sqrt{2}} \sin \delta \sqrt{1 - \frac{3}{2} \sin^2 \theta_{13}}, \quad (4.14)$$

Using  $\sin \theta_{13} \simeq 0.16$  and  $|\sin \delta| > \frac{1}{2}$ , the allowed range  $0.026 < |J_{\text{CP}}| < 0.036$  is obtained.

Fig.3, shows the variation of neutrino parameters like solar mixing angle ( $\theta_{12}$ ), reactor mixing angle ( $\theta_{13}$ ), and atmospheric mixing angle ( $\theta_{23}$ ) along with the Jarlskog rephrasing invariant  $J_{\text{CP}}$  with the change of internal mixing angle  $\theta$ . The solid green line represents  $\theta_{12}$ , solid blue line is for  $\theta_{23}$  and solid magenta line is for  $\theta_{13}$  while dashed lines show different predictions for rephrasing invariant  $J_{\text{CP}}$  by fixing phase  $\delta = 0, 60, 100$  for yellow, magenta and green respectively. The experimentally measured  $\sigma$  allowed region for  $\theta_{23}, \theta_{12}$  and  $\theta_{13}$  [72] are displayed in blue, green and magenta bands respectively. We have done random scan of internal mixing angle  $\theta$  and the phase angle  $\delta$  in the range  $0-2\pi$  by fixing  $M_1$  at 25 GeV,  $M_2$  at 800 GeV and  $M_3$  at 2 TeV, and considered only those values which fall within the experimental range and shown the correlation between predicted neutrino oscillation parameters in Fig.4.

## 5 Non-unitarity effects in linear seesaw

The linear seesaw mechanism allows large mixing between light and heavy neutrinos, which gives dominant contributions to lepton flavor violating decays and Jarlskog invariants  $\mathbf{J}_{\text{CP}}$ . These processes are related to non-unitarity effects in neutrino masses and mixing. [73–84]

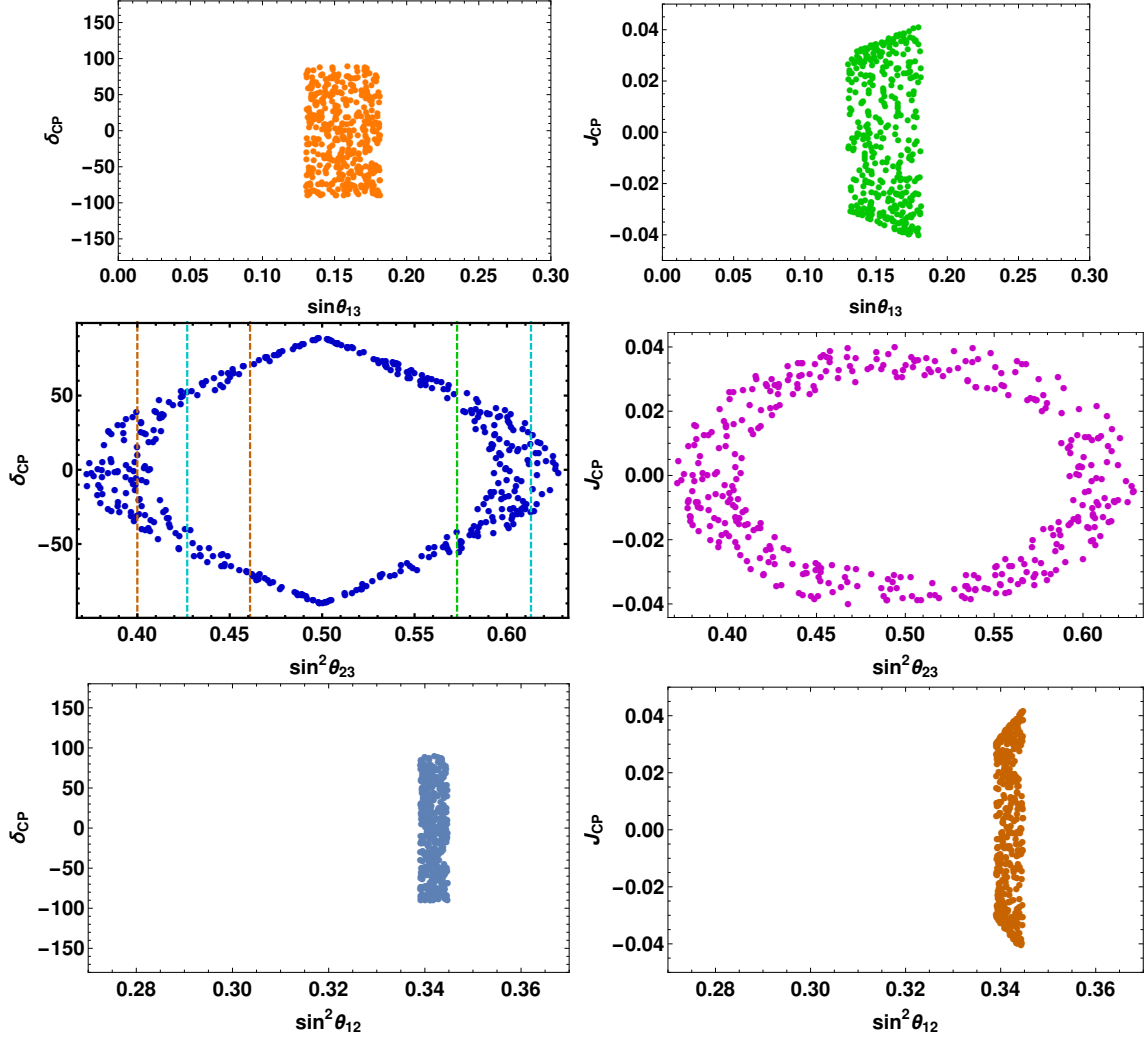


Figure 4: The plots show the inter-relationship between the Dirac CP violating phase  $\delta_{CP}$  and rephrasing invariant  $J_{CP}$  with other mixing angles  $\theta_{12}$ ,  $\theta_{23}$ ,  $\theta_{13}$ .

The complete neutral fermion spectrum with flavor and mass eigenstates are related in the following way

$$|\Psi\rangle_f = \mathbb{V}^\dagger |\Psi\rangle_m \quad , \quad |\Psi\rangle_f = \begin{pmatrix} \nu_L \\ \nu_R^c \\ S_L \end{pmatrix} \quad , \quad |\Psi\rangle_m = \begin{pmatrix} \nu_i \\ N_k \end{pmatrix} \quad (5.1)$$

Here we assume  $\nu_L$  with  $L = e, \mu, \tau$  for flavour eigenstates,  $\nu_i$  with  $i = 1, 2, 3$  for mass eigenstates,  $\nu_R^c$  and  $S_L$  as flavour eigenstates,  $N_k$  with  $k = 1, 2, \dots, 6$  for mass eigenstates. After complete diagonalization process the physical neutral fermions are comprised of three Majorana neutrinos and three Dirac neutrinos which come up after six heavy neutrinos pair



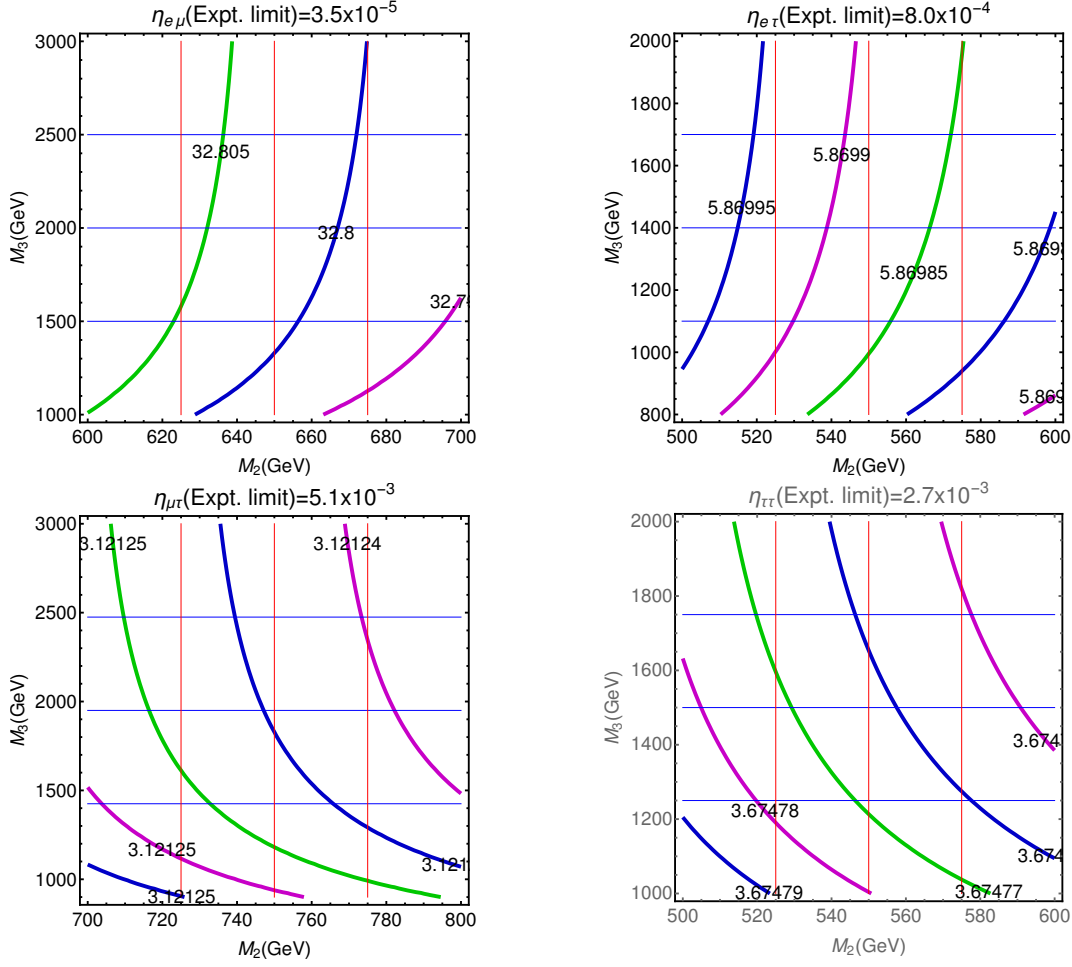


Figure 5: Contours plots in the plane of  $M_2$  and  $M_3$  for different fixed values of  $M_1$  by saturating the experimental values of unitarity violating parameter  $\eta$  in  $e\mu$ ,  $e\tau$ ,  $\mu\tau$ ,  $\tau\tau$  sectors.

up. The mass formula for light as well as heavy neutrinos are given by

$$\begin{aligned}
 m_\nu &\simeq m_{LR} m_{RS}^{-1} m_{LS}^T + \text{transpose} \\
 M &\simeq m_{RS} + \dots
 \end{aligned}
 \tag{5.2}$$

The complete  $9 \times 9$  mixing matrix is of the following form [14],

$$\mathbb{V} = \mathbb{W} \cdot \mathbb{U} = \begin{pmatrix} \sqrt{1 + X X^\dagger} U_\nu & X U_N \\ X^\dagger U_\nu & \sqrt{1 + X^\dagger X} U_N \end{pmatrix} \cdot \begin{pmatrix} U_\nu & 0 \\ 0 & U_N \end{pmatrix}$$

The unitary mixing matrices  $U_\nu$  and  $U_N$  are required to diagonalise the light neutrino mass matrix  $m_\nu$  and heavy neutrino mass matrix  $M$ . In usual case, the light active Majorana neutrino mass matrix is diagonalized by the PMNS mixing matrix  $U_{\text{PMNS}}$  as  $U_{\text{PMNS}}^\dagger m_\nu U_{\text{PMNS}}^* = \text{diag}(m_1, m_2, m_3)$  where  $m_1, m_2, m_3$  are mass eigenvalues for light neutrinos. However, due to the presence of extra heavy neutrinos, the diagonalizing mixing matrix in case of linear seesaw

mechanism [75–77, 85](where the neutral lepton sector comprises of light active Majorana neutrinos plus two right-handed sterile neutrinos) is no longer unitary and is given by,

$$\mathbb{N} = (1 - \eta) U_\nu \equiv (1 - \eta) U_{\text{PMNS}}, \quad (5.3)$$

Here,  $\eta$  is a measure of deviation from unitarity in the PMNS mixing matrix in the light neutrino sector. The non-unitarity effect can be recast in terms of  $m_{LR}$  and  $m_{RS}$  as [76],

$$\eta = \frac{1}{2} m_{LR}^* m_{RS}^\dagger - 1 m_{RS}^{-1} m_{LR}^T. \quad (5.4)$$

In linear seesaw scheme invoked with  $A_4$  flavor symmetry, the structure of  $m_{LR}$  and  $m_{LS}$  are proportional to the identity matrix and the other matrix  $m_{RS}$  is diagonalized in the following way

$$m_{RS}^d = \left( U_{\text{TBM}} U_{13} \right)^T m_{RS} \left( U_{\text{TBM}} U_{13} \right) \quad (5.5)$$

where,

$$U_{\text{TBM}} U_{13} = \begin{pmatrix} \frac{2}{\sqrt{6}} \cos \theta & \frac{1}{\sqrt{3}} & \frac{2}{\sqrt{6}} \sin \theta e^{-i\delta} \\ -\frac{1}{\sqrt{6}} \cos \theta + \frac{1}{\sqrt{2}} \sin \theta e^{i\delta} & \frac{1}{\sqrt{3}} & -\frac{1}{\sqrt{6}} \sin \theta e^{-i\delta} - \frac{1}{\sqrt{2}} \cos \theta \\ -\frac{1}{\sqrt{6}} \cos \theta - \frac{1}{\sqrt{2}} \sin \theta e^{i\delta} & \frac{1}{\sqrt{3}} & -\frac{1}{\sqrt{6}} \sin \theta e^{-i\delta} + \frac{1}{\sqrt{2}} \cos \theta \end{pmatrix}$$

$$m_{RS}^d = \begin{pmatrix} M_1 & 0 & 0 \\ 0 & M_2 & 0 \\ 0 & 0 & M_3 \end{pmatrix} \quad (5.6)$$

The linear seesaw formula provides sub-eV scale (of order 0.1 eV) masses for light active neutrinos with values of model parameters,  $m_{LR} \sim 0.5$  GeV,  $m_{RS} \sim 10^3$  GeV and  $m_{LS} \sim 100$  eV. The unitarity violation in  $e\mu, e\tau, \mu\tau, \tau\tau$  sector can be expressed by saturating the experimental bound which are  $|\eta_{e\mu}| < 3.5 \times 10^{-5}$ ,  $|\eta_{e\tau}| < 8.0 \times 10^{-4}$ ,  $|\eta_{\mu\tau}| < 5.1 \times 10^{-3}$  and  $|\eta_{\tau\tau}| < 2.7 \times 10^{-3}$  [35, 86, 87] as

$$\begin{aligned} \boldsymbol{\eta}_{e\mu} &= m_d^2 \times \left[ \frac{1}{M_1^2} \left( \sqrt{\frac{2}{3}} \cos \theta \left( \frac{-\cos \theta}{\sqrt{6}} + \frac{\cos \delta \sin \theta}{\sqrt{2}} + \frac{i \sin \delta \sin \theta}{\sqrt{2}} \right) \right) + \frac{1}{3M_2^2} \right. \\ &\quad \left. + \frac{1}{M_3^2} \left( \sqrt{\frac{2}{3}} \cos \delta \sin \theta - i \sqrt{\frac{2}{3}} \sin \delta \sin \theta \right) \left( \frac{-\cos \theta}{\sqrt{2}} - \frac{\cos \delta \sin \theta}{\sqrt{6}} + \frac{i \sin \delta \sin \theta}{\sqrt{6}} \right) \right] \quad (5.7) \end{aligned}$$

$$\begin{aligned} \boldsymbol{\eta}_{e\tau} &= m_d^2 \times \left[ \frac{1}{M_1^2} \left( \sqrt{\frac{2}{3}} \cos \theta \left( \frac{-\cos \theta}{\sqrt{6}} - \frac{\cos \delta \sin \theta}{\sqrt{2}} + \frac{i \sin \delta \sin \theta}{\sqrt{2}} \right) \right) + \frac{1}{3M_2^2} \right. \\ &\quad \left. + \frac{1}{M_3^2} \left( \sqrt{\frac{2}{3}} \cos \delta \sin \theta - i \sqrt{\frac{2}{3}} \sin \delta \sin \theta \right) \left( \frac{\cos \theta}{\sqrt{2}} - \frac{\cos \delta \sin \theta}{\sqrt{6}} - \frac{i \sin \delta \sin \theta}{\sqrt{6}} \right) \right] \quad (5.8) \end{aligned}$$

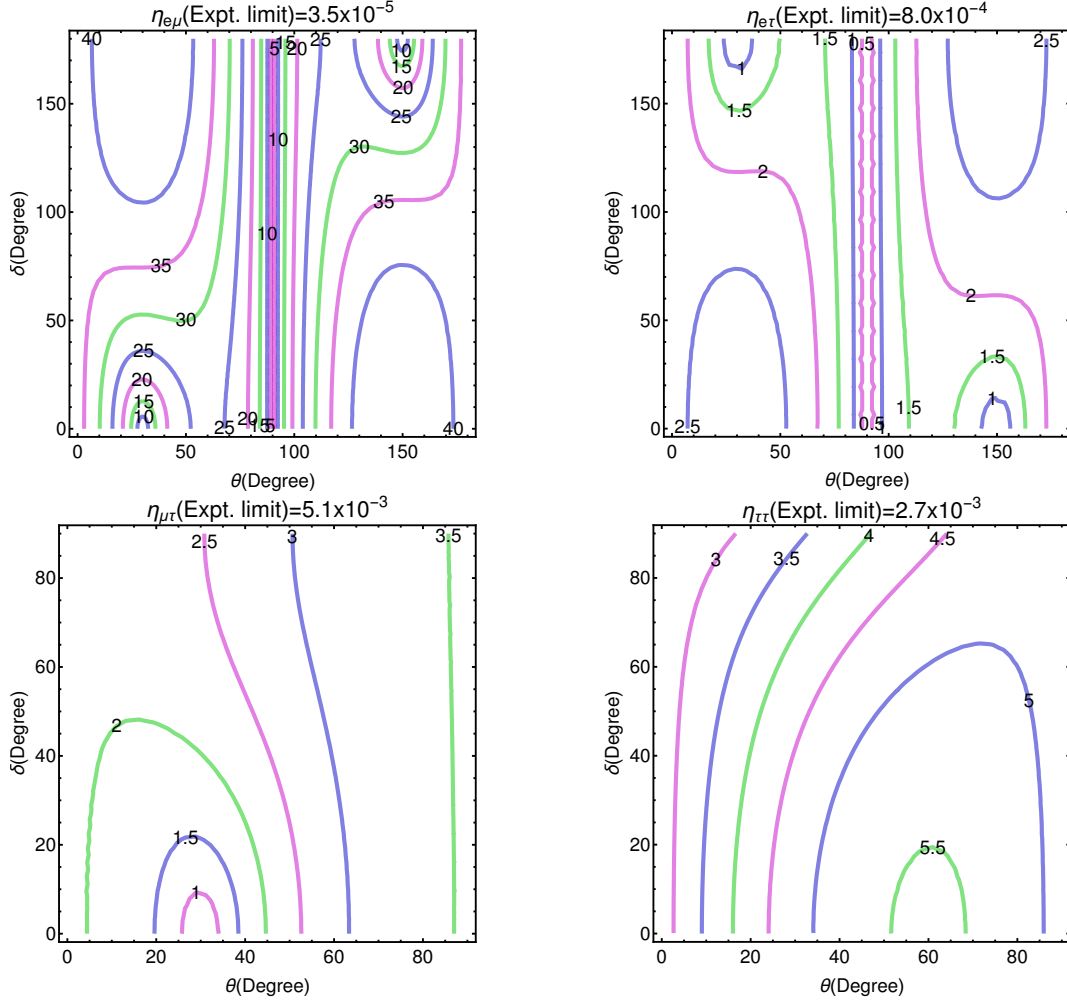


Figure 6: Correlation plot between the internal mixing angle  $\theta$  and phase  $\delta$  for observable unitarity effects at current and planned experiments in  $e\mu, e\tau, \mu\tau, \tau\tau$  sectors.

$$\begin{aligned}
 \eta_{\mu\tau} = & m_d^2 \times \left[ \frac{1}{M_1^2} \left( \left( \frac{-\cos\theta}{\sqrt{6}} - \frac{\cos\delta \sin\theta}{\sqrt{2}} + \frac{i \sin\delta \sin\theta}{\sqrt{2}} \right) \left( \frac{-\cos\theta}{\sqrt{6}} + \frac{\cos\delta \sin\theta}{\sqrt{2}} + \frac{i \sin\delta \sin\theta}{\sqrt{2}} \right) \right) + \frac{1}{3M_2^2} \right. \\
 & \left. + \frac{1}{M_3^2} \left( \frac{\cos\theta}{\sqrt{2}} - \frac{\cos\delta \sin\theta}{\sqrt{6}} - \frac{i \sin\delta \sin\theta}{\sqrt{6}} \right) \left( \frac{-\cos\theta}{\sqrt{2}} - \frac{\cos\delta \sin\theta}{\sqrt{6}} + \frac{i \sin\delta \sin\theta}{\sqrt{6}} \right) \right] \quad (5.9)
 \end{aligned}$$

$$\begin{aligned}
 \eta_{\tau\tau} = & m_d^2 \times \left[ \frac{1}{M_1^2} \left( \left( \frac{-\cos\theta}{\sqrt{6}} - \frac{\cos\delta \sin\theta}{\sqrt{2}} - \frac{i \sin\delta \sin\theta}{\sqrt{2}} \right) \left( \frac{-\cos\theta}{\sqrt{6}} - \frac{\cos\delta \sin\theta}{\sqrt{2}} + \frac{i \sin\delta \sin\theta}{\sqrt{2}} \right) \right) + \frac{1}{3M_2^2} \right. \\
 & \left. + \frac{1}{M_3^2} \left( \frac{\cos\theta}{\sqrt{2}} - \frac{\cos\delta \sin\theta}{\sqrt{6}} - \frac{i \sin\delta \sin\theta}{\sqrt{6}} \right) \left( \frac{\cos\theta}{\sqrt{2}} - \frac{\cos\delta \sin\theta}{\sqrt{6}} + \frac{i \sin\delta \sin\theta}{\sqrt{6}} \right) \right] \quad (5.10)
 \end{aligned}$$

In Fig.5 we have used experimental values of  $\eta$  in the  $e\mu, e\tau, \mu\tau, e\tau\tau$  sectors [35, 86, 87] and plotted  $M_3$  versus  $M_2$  where the curves show the allowed values of  $M_1$ . We have used the

equations 5.7, 5.8, 5.9, 5.10 for the four plots and set  $\theta = 120$  degree,  $\delta = 60$  degree. Whereas in Fig.6 we have fixed  $M_2$  at 100 GeV,  $M_3$  at 2 TeV and plotted  $\delta$  versus  $\theta$  for observable  $\eta$  at experiments.

## 6 Low Energy Lepton Flavour Violating Processes

The observation of neutrino oscillations strongly hints that lepton flavor violation might be occurring in other processes as well. In our model, the mechanism of Majorana neutrino mass generation is associated with the occurrence of charged lepton flavor violation (LFV). LFV is highly suppressed by GIM mechanism, that is,  $(\Delta m_\nu^2/m_W^2) \approx 10^{-50}$  and is well below any experimental sensitivity in case only light neutrinos contribute to them. However, in the considered left-right symmetric framework due to the contribution from heavy right-handed neutrinos sizable charged lepton flavor violation occurs. For a discussion we focus here on low energy LFV processes  $\mu \rightarrow e\gamma$ ,  $\mu \rightarrow eee$  and  $\mu \rightarrow e$  conversion in nuclei because of their sensitivity and omit LFV  $\tau$  decays. For a review of LFV and new physics scenarios, one may refer [88].

As discussed in the previous section, unitarity violation has implications on prediction for lepton flavor violation. Since the measure of unitarity violation is of the order of  $M_{LR}^2/M^2$ ,  $\mu \rightarrow e\gamma$  term plays a vital role in deriving constraints on input parameters like internal mixing angle  $\theta$  and phases  $\delta$ . The branching ratio for this particular process  $\mu \rightarrow e\gamma$  is given by [89]

$$\text{BR}(\mu \rightarrow e\gamma) = \frac{3\alpha}{32\pi} \sum_{i=1}^3 f\left(\frac{M_i}{M_W}\right) |\Theta_{\mu i}^* \Theta_{ei}|^2, \quad (6.1)$$

Here,  $M_i$  denotes for physical masses for pseudo-Dirac neutrinos, the other loop factor  $f(M_i^2/M_W^2)$  is the order of one and this results,

$$\text{BR}(\mu \rightarrow e\gamma) \simeq 8.4 \times 10^{-14} \cdot \left(\frac{|(\Theta\Theta^\dagger)_{e\mu}|}{10^{-5}}\right)^2. \quad (6.2)$$

We examined how the input model parameters are correlated by saturating the experimental bounds on these LFV processes. The term  $\Theta_{\alpha i} \Theta_{\beta i}^\dagger \simeq \boldsymbol{\eta}_{\alpha\beta}$  in the above equation represents deviation of unitarity in the lepton sector which has been discussed in previous section. It has also been demonstrated in contour plots in the plane of internal mixing angle  $\theta$  and phase  $\delta$  in Fig.7.

Left-right symmetric model with linear seesaw mechanism can mediate other LFV processes like  $Br(\mu \rightarrow eee)$  and conversion rate process  $R^N(\mu \rightarrow e)$  in a nucleus which is discussed

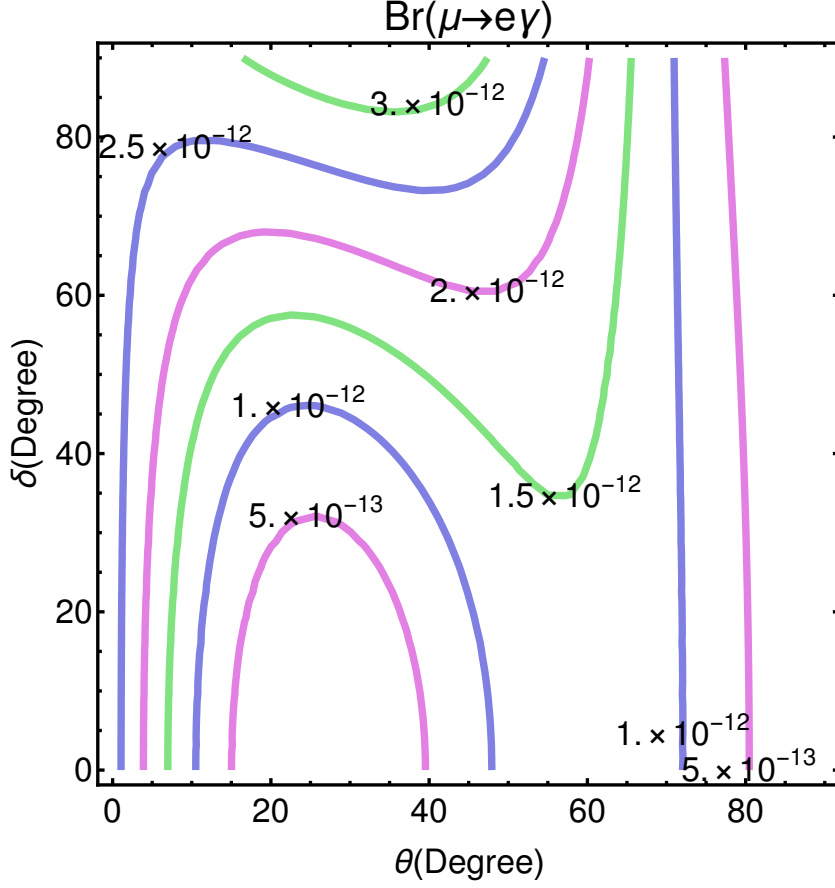


Figure 7: Correlation plot between the internal mixing angle  $\theta$  and phase  $\delta$  for branching ratios for the lepton flavour violating processes,  $BR(\mu \rightarrow e\gamma)$ .

in reference [21]. The experimental bounds on these LFV processes are as follows [90–93],

$$\begin{aligned}
 Br_{\text{exp}}(\mu \rightarrow e\gamma) &< 5.7 \cdot 10^{-13}, \\
 R_{\text{exp}}^{Au}(\mu \rightarrow e) &< 8.0 \cdot 10^{-13}, \\
 Br_{\text{exp}}(\mu \rightarrow eee) &< 1.0 \cdot 10^{-12}.
 \end{aligned}
 \tag{6.3}$$

At present the process  $Br(\mu \rightarrow eee)$  gives the most restrictive bound while the currently running MEG experiment [90,94] may provide a better sensitivity with

$$Br_{\text{MEG}}(\mu \rightarrow e\gamma) \approx 10^{-13},
 \tag{6.4}$$

Other planned experiments like COMET and Mu2e aim to reach [95,96]

$$R_{\text{COMET}}^{Al}(\mu \rightarrow e) \approx 10^{-16}.
 \tag{6.5}$$

In Fig.7 we have presented a correlation plot between the internal mixing angle  $\theta$  and phase  $\delta$  by fixing  $M_1, M_2$  and  $M_3$  at 35 GeV, 100 GeV and 2 TeV respectively for branching ratios

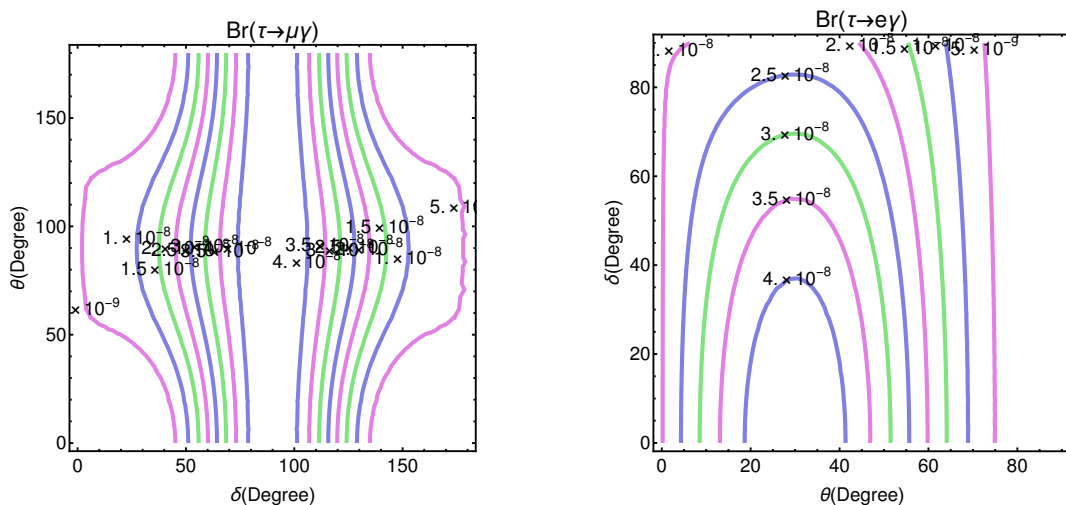


Figure 8: Correlation plot between the internal mixing angle  $\theta$  and phase  $\delta$  for branching ratios for the lepton flavour violating processes like  $\text{BR}(\tau \rightarrow e\gamma)$  and  $\text{BR}(\tau \rightarrow \mu\gamma)$ .

for the LFV process ( $\mu \rightarrow e\gamma$ ). The curves in the plot represent different allowed values of branching ratios for the process for different values of  $\delta$  and  $\theta$ . It is seen that the values are sensitive to the current experimental bound on branching ratio as mentioned in eq.6.3. Similarly in Fig.8 we have shown correlation plots between  $\theta$  and  $\delta$  for branching ratios of the processes ( $\tau \rightarrow e\gamma$ ) and ( $\tau \rightarrow \mu\gamma$ ) by fixing  $M_1, M_2$  and  $M_3$  at 2.5 GeV, 100 GeV and 2 TeV respectively .

## 7 CP-violation for active neutrinos via Jarlskog invariants

The CP-violating effects in neutrino oscillation are studied mostly in various long-baseline experiments with neutrinos  $\nu_\mu$  and anti-neutrinos  $\bar{\nu}_\mu$ . This effect is characterized by the PMNS mixing matrix  $\mathbb{N}$  containing non-unitarity information rather than the  $U_{\text{PMNS}}$  matrix through Jarlskog invariant [71, 97]. They measure the strength of leptonic CP-violation in neutrino oscillations. Using usual PMNS mixing matrix  $U_{\text{PMNS}} \equiv U$ , the standard contribution to these CP-violating effects is determined by the rephasing invariant  $J_{\text{CP}}$  associated with the Dirac phase  $\delta_{\text{CP}}$  and matrix elements of the PMNS matrix

$$J_{\text{CP}} \equiv \text{Im} (U_{\alpha i} U_{\beta j} U_{\alpha j}^* U_{\beta i}^*) = \cos \theta_{12} \cos^2 \theta_{13} \cos \theta_{23} \sin \theta_{12} \sin \theta_{13} \sin \theta_{23} \sin \delta_{\text{CP}}.$$

However, in extended seesaw schemes like linear seesaw mechanism which we follow, the leptonic CP-violation can be written in terms of  $\mathbb{N}$  as,

$$\mathcal{J}_{\alpha\beta}^{ij} = \text{Im} (\mathbb{N}_{\alpha i} \mathbb{N}_{\beta j} \mathbb{N}_{\alpha j}^* \mathbb{N}_{\beta i}^*) \simeq J_{\text{CP}} + \Delta J_{\alpha\beta}^{ij} \quad (7.1)$$

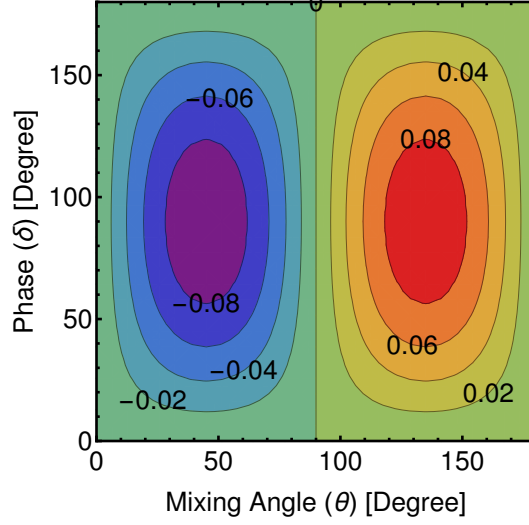


Figure 9: Plot showing relation between internal mixing angle  $\theta$  and phase angle  $\delta$  while fixing the rephasing invariant  $J_{CP}$  within observable range.

Here the indices  $\alpha \neq \beta$  run over  $e, \mu, \tau$  while indices  $i, j$  run over  $1, 2, 3$ . Assuming  $\sin \theta_{13}$  small and non-unitarity parameter  $\eta$  (up to second order), the derived expression for  $\Delta J_{\alpha\beta}^{ij}$  is given by [35]

$$\Delta J_{\alpha\beta}^{ij} = - \sum_{\gamma=e,\mu,\tau} \text{Im} \left[ \eta_{\alpha\gamma} U_{\gamma i} U_{\beta j} U_{\alpha j}^* U_{\beta i}^* + \eta_{\beta\gamma} U_{\alpha i} U_{\gamma j} U_{\alpha j}^* U_{\beta i}^* + \eta_{\alpha\gamma}^* U_{\alpha i} U_{\beta j} U_{\gamma j}^* U_{\beta j}^* + \eta_{\beta\gamma}^* U_{\alpha i} U_{\beta j} U_{\alpha j}^* U_{\gamma j}^* \right]. \quad (7.2)$$

Table.2 shows the extra contributions to  $\Delta J_{\alpha\beta}^{ij}$  due to unitary violation in the neutrino sector. This has been worked out by choosing different values of  $M_1, M_2, M_3$  while fixing  $\theta$  and  $\delta$  and following the mass hierarchy for linear seesaw mechanism i.e,  $m_{RS} \gg m_{LR} \gg m_{LS}$ .

M	$\Delta J_{e\mu}^{12}$	$\Delta J_{\mu\tau}^{12}$	$\Delta J_{e\tau}^{13}$	$\Delta J_{e\tau}^{23}$	$\Delta J_{\mu\tau}^{13}$
(a)	$2.77 \times 10^{-6}$	$7.2 \times 10^{-5}$	$-1.62 \times 10^{-5}$	$-2.4 \times 10^{-5}$	$-7.2 \times 10^{-5}$
(b)	$2.8 \times 10^{-6}$	$5.54 \times 10^{-6}$	$-5.86 \times 10^{-7}$	$-1.01 \times 10^{-6}$	$-5.54 \times 10^{-4}$
(c)	$1.38 \times 10^{-6}$	$1.38 \times 10^{-6}$	$1.38 \times 10^{-6}$	$-1.38 \times 10^{-6}$	$-1.38 \times 10^{-6}$

Table 2: Estimated CP-violating effects for three cases, (a)  $M = (10, 50, 1500)$  GeV, (b) partially degenerate masses  $M = (50, 50, 1000)$  GeV and (c) fully degenerate masses  $M = (500, 500, 500)$  GeV. We have fixed the internal mixing angle and phase  $\delta$  as 120 degree and 60 degree, respectively.

The numerical results for relation between the internal mixing angle  $\theta$  and the phase  $\delta$  are displayed in Fig.9 and 10. In Fig.9 the range for the value of  $J_{CP}$  comes out to be 0.02 to 0.04 which matches with the experimental observable range. Since  $J_{CP}$  has a modulus, both

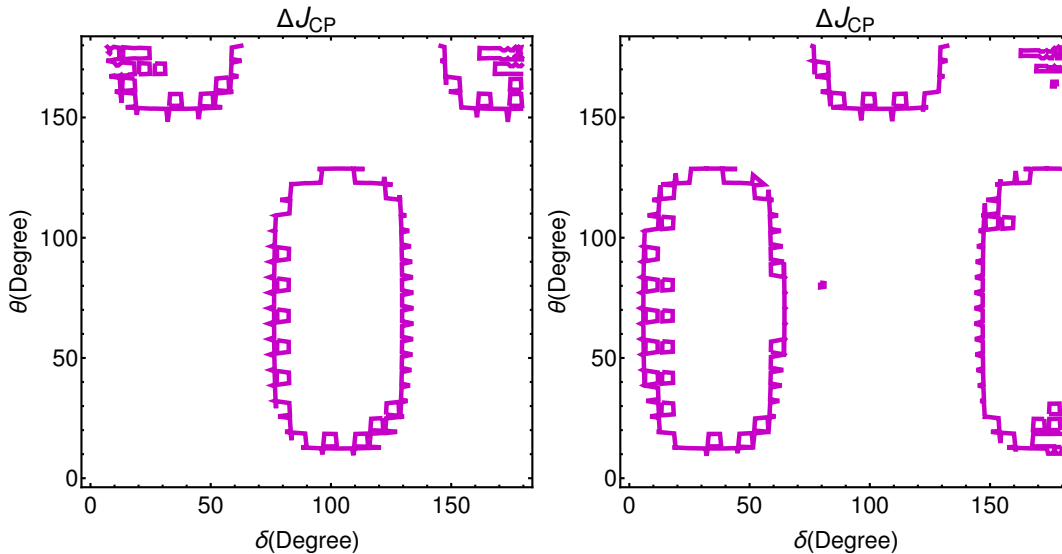


Figure 10: The contour plot for the rephasing invariant  $\Delta J_{e\mu}^{12}$  due to unitary violation in the neutrino sector in the plane of internal mixing angle  $\theta$  and internal phase angle  $\delta$ . The value of  $\Delta J_{e\mu}^{12}$  are considered here around  $10^{-6}$  by taking degenerate values of  $M_1, M_2, M_3$ .

negative and positive values are shown in the figure. In Fig.10 the value of  $\Delta J_{e\mu}^{12}$  lies around  $10^{-6}$  for degenerate values of  $M_1, M_2, M_3$ . The allowed range of rephasing invariant  $J_{CP}$  is  $0.026 < |J_{CP}| < 0.036$  and that of  $\Delta J_{CP}$  is  $10^{-5} < |\Delta J_{CP}| < 10^{-7}$ .

## 8 Conclusion

We have studied a left-right symmetric model with discrete  $A_4$ -flavour symmetry where neutrino masses and mixing are explained via linear seesaw mechanism. Even though  $A_4$  flavour based models have been studied before, we have shown here that the  $A_4$  extension of LRSM simpler analytical expressions for large non-unitarity effect which can lead to dominant contributions to LFV decays. We have shown correlation among model parameters like internal mixing angle  $\theta$ , internal phase  $\delta$  and their dependence on experimentally determined parameters like mixing angles  $\theta_{12}, \theta_{23}, \theta_{13}$  and sum of neutrino masses both analytically as well as numerically.

The model facilitates sizable charged lepton flavour violation due to contributions from heavy right handed neutrinos. We have studied non-unitarity effects in linear seesaw which has implications on prediction for LFV decays like  $\mu \rightarrow e\gamma, \mu \rightarrow eee$  and  $\mu \rightarrow e$  and by saturating the experimental bounds on these decays we have derived constraints on input model parameters. Finally we have studied CP-violation for active neutrinos via Jarlskog invariants and shown extra contributions to CP violating effects that the model generates



due to unitarity violation in the neutrino sector. Again by saturating the experimental values of unitarity violating parameter  $\eta$  in  $e\mu, e\tau, \mu\tau, \tau\tau$  sectors we have generated contour plots to show constraints on model parameters. Interestingly, the range for the value of  $J_{CP}$  comes out to be 0.02 to 0.04 which matches with the experimental observable range.

## 9 Acknowledgement

Purushottam Sahu would like to acknowledge Ministry of Human Resource Development (MHRD), Govt of India for financial support.

## References

- [1] R. N. Mohapatra and J. C. Pati, “A Natural Left-Right Symmetry,” *Phys. Rev.* **D11** (1975) 2558.
- [2] J. C. Pati and A. Salam, “Lepton Number as the Fourth Color,” *Phys. Rev.* **D10** (1974) 275–289. [Erratum: *Phys. Rev.* **D11**, 703(1975)].
- [3] G. Senjanovic and R. N. Mohapatra, “Exact Left-Right Symmetry and Spontaneous Violation of Parity,” *Phys. Rev.* **D12** (1975) 1502.
- [4] G. Senjanovic, “Spontaneous Breakdown of Parity in a Class of Gauge Theories,” *Nucl. Phys.* **B153** (1979) 334–364.
- [5] R. N. Mohapatra and G. Senjanovic, “Neutrino Masses and Mixings in Gauge Models with Spontaneous Parity Violation,” *Phys. Rev.* **D23** (1981) 165.
- [6] E. K. Akhmedov, M. Lindner, E. Schnapka, and J. W. F. Valle, “Dynamical left-right symmetry breaking,” *Phys. Rev.* **D53** (1996) 2752–2780, [[hep-ph/9509255](#)].
- [7] J. Heeck and S. Patra, “Minimal Left-Right Symmetric Dark Matter,” *Phys. Rev. Lett.* **115** no. 12, (2015) 121804, [[1507.01584](#)].
- [8] C. Garcia-Cely and J. Heeck, “Phenomenology of left-right symmetric dark matter,” [[1512.03332](#)]. [[JCAP1603,021\(2016\)](#)].
- [9] S. Patra and S. Rao, “Singlet fermion Dark Matter within Left-Right Model,” *Phys. Lett.* **B759** (2016) 454–458, [[1512.04053](#)].
- [10] S. Patra, “Dark matter, lepton and baryon number, and left-right symmetric theories,” *Phys. Rev.* **D93** no. 9, (2016) 093001, [[1512.04739](#)].

- [11] P. Minkowski, “ $\mu \rightarrow e\gamma$  at a Rate of One Out of  $10^9$  Muon Decays?,” *Phys. Lett.* **67B** (1977) 421–428.
- [12] R. N. Mohapatra and G. Senjanovic, “Neutrino Mass and Spontaneous Parity Nonconservation,” *Phys. Rev. Lett.* **44** (1980) 912. [,231(1979)].
- [13] C.-H. Lee, P. S. Bhupal Dev, and R. N. Mohapatra, “Natural TeV-scale left-right seesaw mechanism for neutrinos and experimental tests,” *Phys. Rev.* **D88** no. 9, (2013) 093010, [1309.0774].
- [14] N. R. Agostinho, G. C. Branco, P. M. F. Pereira, M. N. Rebelo, and J. I. Silva-Marcos, “Can one have significant deviations from leptonic  $3 \times 3$  unitarity in the framework of type I seesaw mechanism?,” *Eur. Phys. J.* **C78** no. 11, (2018) 895, [1711.06229].
- [15] M. Magg and C. Wetterich, “Neutrino Mass Problem and Gauge Hierarchy,” *Phys. Lett.* **94B** (1980) 61–64.
- [16] J. Schechter and J. W. F. Valle, “Neutrino Masses in  $SU(2) \times U(1)$  Theories,” *Phys. Rev.* **D22** (1980) 2227.
- [17] T. P. Cheng and L.-F. Li, “Neutrino Masses, Mixings and Oscillations in  $SU(2) \times U(1)$  Models of Electroweak Interactions,” *Phys. Rev.* **D22** (1980) 2860.
- [18] G. Lazarides, Q. Shafi, and C. Wetterich, “Proton Lifetime and Fermion Masses in an  $SO(10)$  Model,” *Nucl. Phys.* **B181** (1981) 287–300.
- [19] P. S. B. Dev and R. N. Mohapatra, “TeV Scale Inverse Seesaw in  $SO(10)$  and Leptonic Non-Unitarity Effects,” *Phys. Rev.* **D81** (2010) 013001, [0910.3924].
- [20] R. N. Mohapatra *et al.*, “Theory of neutrinos: A White paper,” *Rept. Prog. Phys.* **70** (2007) 1757–1867, [hep-ph/0510213].
- [21] V. Cirigliano, A. Kurylov, M. J. Ramsey-Musolf, and P. Vogel, “Lepton flavor violation without supersymmetry,” *Phys. Rev.* **D70** (2004) 075007, [hep-ph/0404233].
- [22] V. Cirigliano, A. Kurylov, M. J. Ramsey-Musolf, and P. Vogel, “Neutrinoless double beta decay and lepton flavor violation,” *Phys. Rev. Lett.* **93** (2004) 231802, [hep-ph/0406199].
- [23] Riazuddin, R. E. Marshak, and R. N. Mohapatra, “Majorana Neutrinos and Low-energy Tests of Electroweak Models,” *Phys. Rev.* **D24** (1981) 1310–1317.

- [24] P. B. Pal, “Constraints on a Muon - Neutrino Mass Around 100-keV,” *Nucl. Phys.* **B227** (1983) 237–251.
- [25] R. N. Mohapatra, “Rare decays of the tau lepton as a probe of the left-right symmetric theories of weak interactions,” *Phys. Rev.* **D46** (1992) 2990–2995.
- [26] F. F. Deppisch, C. Hati, S. Patra, P. Pritimita, and U. Sarkar, “Neutrinoless double beta decay in left-right symmetric models with a universal seesaw mechanism,” *Phys. Rev.* **D97** no. 3, (2018) 035005, [1701.02107].
- [27] C. Hati, S. Patra, P. Pritimita, and U. Sarkar, “Neutrino Masses and Leptogenesis in Left-Right Symmetric Models: A Review From a Model Building Perspective,” *Front.in Phys.* **6** (2018) 19.
- [28] P. Pritimita, N. Dash, and S. Patra, “Neutrinoless Double Beta Decay in LRSM with Natural Type-II seesaw Dominance,” *JHEP* **10** (2016) 147, [1607.07655].
- [29] S.-F. Ge and W. Rodejohann, “JUNO and Neutrinoless Double Beta Decay,” *Phys. Rev.* **D92** no. 9, (2015) 093006, [1507.05514].
- [30] F. F. Deppisch, T. E. Gonzalo, S. Patra, N. Sahu, and U. Sarkar, “Double beta decay, lepton flavor violation, and collider signatures of left-right symmetric models with spontaneous  $D$ -parity breaking,” *Phys. Rev.* **D91** no. 1, (2015) 015018, [1410.6427].
- [31] V. Tello, M. Nemevsek, F. Nesti, G. Senjanovic, and F. Vissani, “Left-Right Symmetry: from LHC to Neutrinoless Double Beta Decay,” *Phys. Rev. Lett.* **106** (2011) 151801, [1011.3522].
- [32] F. F. Deppisch, T. E. Gonzalo, S. Patra, N. Sahu, and U. Sarkar, “Signal of Right-Handed Charged Gauge Bosons at the LHC?,” *Phys. Rev.* **D90** no. 5, (2014) 053014, [1407.5384].
- [33] S. Patra and P. Pritimita, “Post-sphaleron baryogenesis and  $n - \bar{n}$  oscillation in non-SUSY SO(10) GUT with gauge coupling unification and proton decay,” *Eur. Phys. J.* **C74** no. 10, (2014) 3078, [1405.6836].
- [34] D. Borah, S. Patra, and P. Pritimita, “Sub-dominant type-II seesaw as an origin of non-zero  $\theta_{13}$  in SO(10) model with TeV scale  $Z'$  gauge boson,” *Nucl. Phys.* **B881** (2014) 444–466, [1312.5885].
- [35] R. L. Awasthi, M. K. Parida, and S. Patra, “Neutrino masses, dominant neutrinoless double beta decay, and observable lepton flavor violation in left-right models and

- SO(10) grand unification with low mass  $W_R, Z_R$  bosons,” *JHEP* **08** (2013) 122, [1302.0672].
- [36] S. Patra, “Neutrinoless double beta decay process in left-right symmetric models without scalar bidoublet,” *Phys. Rev.* **D87** no. 1, (2013) 015002, [1212.0612].
- [37] J. Chakraborty, H. Z. Devi, S. Goswami, and S. Patra, “Neutrinoless double- $\beta$  decay in TeV scale Left-Right symmetric models,” *JHEP* **08** (2012) 008, [1204.2527].
- [38] P. S. Bhupal Dev, S. Goswami, M. Mitra, and W. Rodejohann, “Constraining Neutrino Mass from Neutrinoless Double Beta Decay,” *Phys. Rev.* **D88** (2013) 091301, [1305.0056].
- [39] J. Barry and W. Rodejohann, “Lepton number and flavour violation in TeV-scale left-right symmetric theories with large left-right mixing,” *JHEP* **09** (2013) 153, [1303.6324].
- [40] M. Nemevsek, F. Nesti, G. Senjanovic, and Y. Zhang, “First Limits on Left-Right Symmetry Scale from LHC Data,” *Phys. Rev.* **D83** (2011) 115014, [1103.1627].
- [41] P. S. Bhupal Dev, C.-H. Lee, and R. N. Mohapatra, “Leptogenesis Constraints on the Mass of Right-handed Gauge Bosons,” *Phys. Rev.* **D90** no. 9, (2014) 095012, [1408.2820].
- [42] W.-Y. Keung and G. Senjanovic, “Majorana Neutrinos and the Production of the Right-handed Charged Gauge Boson,” *Phys. Rev. Lett.* **50** (1983) 1427.
- [43] S. P. Das, F. F. Deppisch, O. Kittel, and J. W. F. Valle, “Heavy Neutrinos and Lepton Flavour Violation in Left-Right Symmetric Models at the LHC,” *Phys. Rev.* **D86** (2012) 055006, [1206.0256].
- [44] S. Bertolini, A. Maiezza, and F. Nesti, “Present and Future K and B Meson Mixing Constraints on TeV Scale Left-Right Symmetry,” *Phys. Rev.* **D89** no. 9, (2014) 095028, [1403.7112].
- [45] G. Beall, M. Bander, and A. Soni, “Constraint on the Mass Scale of a Left-Right Symmetric Electroweak Theory from the K(L) K(S) Mass Difference,” *Phys. Rev. Lett.* **48** (1982) 848.
- [46] S.-F. Ge, M. Lindner, and S. Patra, “New physics effects on neutrinoless double beta decay from right-handed current,” *JHEP* **10** (2015) 077, [1508.07286].

- [47] F. F. Deppisch, L. Graf, S. Kulkarni, S. Patra, W. Rodejohann, N. Sahu, and U. Sarkar, “Reconciling the 2 TeV excesses at the LHC in a linear seesaw left-right model,” *Phys. Rev.* **D93** no. 1, (2016) 013011, [1508.05940].
- [48] M. Hirsch, H. V. Klapdor-Kleingrothaus, and O. Panella, “Double beta decay in left-right symmetric models,” *Phys. Lett.* **B374** (1996) 7–12, [hep-ph/9602306]. [879(1996)].
- [49] P. S. Bhupal Dev and R. N. Mohapatra, “Unified explanation of the  $eejj$ , diboson and dijet resonances at the LHC,” *Phys. Rev. Lett.* **115** no. 18, (2015) 181803, [1508.02277].
- [50] B. Bajc, M. Nemevsek, and G. Senjanovic, “Probing leptonic CP phases in LFV processes,” *Phys. Lett.* **B684** (2010) 231–235, [0911.1323].
- [51] E. Ma and G. Rajasekaran, “Softly broken A(4) symmetry for nearly degenerate neutrino masses,” *Phys. Rev.* **D64** (2001) 113012, [hep-ph/0106291].
- [52] K. S. Babu, E. Ma, and J. W. F. Valle, “Underlying A(4) symmetry for the neutrino mass matrix and the quark mixing matrix,” *Phys. Lett.* **B552** (2003) 207–213, [hep-ph/0206292].
- [53] G. Altarelli and F. Feruglio, “Tri-bimaximal neutrino mixing from discrete symmetry in extra dimensions,” *Nucl. Phys.* **B720** (2005) 64–88, [hep-ph/0504165].
- [54] M. Holthausen, M. Lindner, and M. A. Schmidt, “Lepton flavor at the electroweak scale: A complete  $A_4$  model,” *Phys. Rev.* **D87** no. 3, (2013) 033006, [1211.5143].
- [55] S. F. King, S. Morisi, E. Peinado, and J. W. F. Valle, “Quark-Lepton Mass Relation in a Realistic  $A_4$  Extension of the Standard Model,” *Phys. Lett.* **B724** (2013) 68–72, [1301.7065].
- [56] B. Karmakar and A. Sil, “An  $A_4$  realization of inverse seesaw: neutrino masses,  $\theta_{13}$  and leptonic non-unitarity,” *Phys. Rev.* **D96** no. 1, (2017) 015007, [1610.01909].
- [57] M. Sruthilaya, R. Mohanta, and S. Patra, “ $A_4$  realization of Linear Seesaw and Neutrino Phenomenology,” *Eur. Phys. J.* **C78** no. 9, (2018) 719, [1709.01737].
- [58] S. Morisi, M. Picariello, and E. Torrente-Lujan, “Model for fermion masses and lepton mixing in SO(10) x A(4),” *Phys. Rev.* **D75** (2007) 075015, [hep-ph/0702034].
- [59] E. Ma, “Suitability of A(4) as a Family Symmetry in Grand Unification,” *Mod. Phys. Lett.* **A21** (2006) 2931–2936, [hep-ph/0607190].

- [60] F. Capozzi, E. Di Valentino, E. Lisi, A. Marrone, A. Melchiorri, and A. Palazzo, “Global constraints on absolute neutrino masses and their ordering,” *Phys. Rev.* **D95** no. 9, (2017) 096014, [1703.04471].
- [61] **KATRIN** Collaboration, M. Aker *et al.*, “First operation of the KATRIN experiment with tritium,” [1909.06069].
- [62] P. F. Harrison, D. H. Perkins, and W. G. Scott, “Tri-bimaximal mixing and the neutrino oscillation data,” *Phys. Lett.* **B530** (2002) 167, [hep-ph/0202074].
- [63] P. F. Harrison, D. H. Perkins, and W. G. Scott, “A Redetermination of the neutrino mass squared difference in tri - maximal mixing with terrestrial matter effects,” *Phys. Lett.* **B458** (1999) 79–92, [hep-ph/9904297].
- [64] A. Rashed and A. Datta, “The charged lepton mass matrix and non-zero  $\theta_{13}$  with TeV scale New Physics,” *Phys. Rev.* **D85** (2012) 035019, [1109.2320].
- [65] B. Pontecorvo, “Inverse beta processes and nonconservation of lepton charge,” *Sov. Phys. JETP* **7** (1958) 172–173. [Zh. Eksp. Teor. Fiz.34,247(1957)].
- [66] Z. Maki, M. Nakagawa, and S. Sakata, “Remarks on the unified model of elementary particles,” *Prog. Theor. Phys.* **28** (1962) 870–880. [,34(1962)].
- [67] W. Chao and Y.-j. Zheng, “Relatively Large Theta13 from Modification to the Tri-bimaximal, Bimaximal and Democratic Neutrino Mixing Matrices,” *JHEP* **02** (2013) 044, [1107.0738].
- [68] M. Sruthilaya, S. C, K. N. Deepthi, and R. Mohanta, “Predicting Leptonic CP phase by considering deviations in charged lepton and neutrino sectors,” *New J. Phys.* **17** no. 8, (2015) 083028, [1408.4392].
- [69] S. Mishra, M. Kumar Behera, R. Mohanta, S. Patra, and S. Singirala, “Neutrino Phenomenology and Dark matter in an  $A_4$  flavour extended  $B - L$  model,” [1907.06429].
- [70] I. Sethi and S. Patra, “Phenomenological Study of Type II Seesaw with  $\Delta(27)$  Symmetry,” [1909.01560].
- [71] C. Jarlskog, “A Basis Independent Formulation of the Connection Between Quark Mass Matrices, CP Violation and Experiment,” *Z. Phys.* **C29** (1985) 491–497.

- [72] I. Esteban, M. C. Gonzalez-Garcia, M. Maltoni, I. Martinez-Soler, and T. Schwetz, “Updated fit to three neutrino mixing: exploring the accelerator-reactor complementarity,” *JHEP* **01** (2017) 087, [1611.01514].
- [73] S. Antusch, C. Biggio, E. Fernandez-Martinez, M. B. Gavela, and J. Lopez-Pavon, “Unitarity of the Leptonic Mixing Matrix,” *JHEP* **10** (2006) 084, [hep-ph/0607020].
- [74] S. Antusch, J. P. Baumann, and E. Fernandez-Martinez, “Non-Standard Neutrino Interactions with Matter from Physics Beyond the Standard Model,” *Nucl. Phys.* **B810** (2009) 369–388, [0807.1003].
- [75] S. Antusch, M. Blennow, E. Fernandez-Martinez, and J. Lopez-Pavon, “Probing non-unitary mixing and CP-violation at a Neutrino Factory,” *Phys. Rev.* **D80** (2009) 033002, [0903.3986].
- [76] D. V. Forero, S. Morisi, M. Tortola, and J. W. F. Valle, “Lepton flavor violation and non-unitary lepton mixing in low-scale type-I seesaw,” *JHEP* **09** (2011) 142, [1107.6009].
- [77] E. Fernandez-Martinez, M. B. Gavela, J. Lopez-Pavon, and O. Yasuda, “CP-violation from non-unitary leptonic mixing,” *Phys. Lett.* **B649** (2007) 427–435, [hep-ph/0703098].
- [78] K. Kanaya, “Neutrino Mixing in the Minimal SO(10) Model,” *Prog. Theor. Phys.* **64** (1980) 2278.
- [79] J. Kersten and A. Yu. Smirnov, “Right-Handed Neutrinos at CERN LHC and the Mechanism of Neutrino Mass Generation,” *Phys. Rev.* **D76** (2007) 073005, [0705.3221].
- [80] M. Malinsky, T. Ohlsson, and H. Zhang, “Non-unitarity effects in a realistic low-scale seesaw model,” *Phys. Rev.* **D79** (2009) 073009, [0903.1961].
- [81] G. Altarelli and D. Meloni, “CP violation in neutrino oscillations and new physics,” *Nucl. Phys.* **B809** (2009) 158–182, [0809.1041].
- [82] F. del Aguila and J. A. Aguilar-Saavedra, “Electroweak scale seesaw and heavy Dirac neutrino signals at LHC,” *Phys. Lett.* **B672** (2009) 158–165, [0809.2096].
- [83] F. del Aguila, J. A. Aguilar-Saavedra, and J. de Blas, “Trilepton signals: the golden channel for seesaw searches at LHC,” *Acta Phys. Polon.* **B40** (2009) 2901–2911, [0910.2720].

- [84] A. Cabrera, “Possible Precise Neutrino Unitarity?,” in *2019 European Physical Society Conference on High Energy Physics (EPS-HEP2019) Ghent, Belgium, July 10-17, 2019*. 2019. [1911.03686].
- [85] H. Hettmansperger, M. Lindner, and W. Rodejohann, “Phenomenological Consequences of sub-leading Terms in See-Saw Formulas,” *JHEP* **04** (2011) 123, [1102.3432].
- [86] R. Lal Awasthi and M. K. Parida, “Inverse Seesaw Mechanism in Nonsupersymmetric SO(10), Proton Lifetime, Nonunitarity Effects, and a Low-mass Z’ Boson,” *Phys. Rev. D* **86** (2012) 093004, [1112.1826].
- [87] L. S. Miranda, P. Pasquini, U. Rahaman, and S. Razzaque, “Searching for non-unitary neutrino oscillations in the present T2K and NO $\nu$ A data,” [1911.09398].
- [88] F. F. Deppisch, “Lepton Flavour Violation and Flavour Symmetries,” *Fortsch. Phys.* **61** (2013) 622–644, [1206.5212].
- [89] A. Ibarra, E. Molinaro, and S. T. Petcov, “Low Energy Signatures of the TeV Scale See-Saw Mechanism,” *Phys. Rev. D* **84** (2011) 013005, [1103.6217].
- [90] **MEG** Collaboration, A. Baldini *et al.*, “Search for the lepton flavour violating decay  $\mu^+ \rightarrow e^+ \gamma$  with the full dataset of the meg experiment,” *Eur.Phys.J.C* **76** no. 8, (2016) 434, [1605.05081].
- [91] T. Nomura, H. Okada, and S. Patra, “An inverse seesaw model with  $a_4$ -modular symmetry,” [1912.00379].
- [92] **BaBar** Collaboration, B. Aubert *et al.*, “Searches for lepton flavor violation in the decays  $\tau_{+-} \rightarrow e_{+-} \gamma$  and  $\tau_{+-} \rightarrow \mu_{+-} \gamma$ ,” *Phys.Rev.Lett.* **104** (2010) 021802, [0908.2381].
- [93] **MEG** Collaboration, J. Adam *et al.*, “New constraint on the existence of the  $\mu^+ \rightarrow e^+ \gamma$  decay,” *Phys. Rev. Lett.* **110** (2013) 201801, [1303.0754].
- [94] **MEG** Collaboration, J. Adam *et al.*, “New limit on the lepton-flavour violating decay  $\mu^+ \rightarrow e^+ \gamma$ ,” *Phys. Rev. Lett.* **107** (2011) 171801, [1107.5547].
- [95] R. K. Kutschke, “The Mu2e Experiment at Fermilab,” in *Proceedings, 31st International Conference on Physics in collisions (PIC 2011): Vancouver, Canada, August 28-September 1, 2011*. 2011. [1112.0242].  
<http://lss.fnal.gov/archive/2011/conf/fermilab-conf-11-887-cd.pdf>.



- [96] **COMET** Collaboration, A. Kurup, “The COherent Muon to Electron Transition (COMET) experiment,” *Nucl. Phys. Proc. Suppl.* **218** (2011) 38–43.
- [97] C. Jarlskog, “Commutator of the quark mass matrices in the standard electroweak model and a measure of maximal CP nonconservation,” *Phys. Rev. Lett.* **55** (Sep, 1985) 1039–1042. <https://link.aps.org/doi/10.1103/PhysRevLett.55.1039>.